THE GEOLOGICAL SOCIETY OF AMERICA®

Permian–Middle Triassic floral succession in North China and implications for the great transition of continental ecosystems

Wenchao Shu[1], Jinnan Tong[1,†], Jianxin Yu[1,†], Jason Hilton[2], Michael J. Benton[3], Xiao Shi[4], José B. Diez[5], Paul B. Wignall[6], Daoliang Chu[1], Li Tian[1], Zhixing Yi[1], and Yongdong Mao[7]

[1]*State Key Laboratory of Biogeology and Environmental Geology, School of Earth Sciences, China University of Geosciences, Wuhan 430074, China*

[2]*School of Geography, Earth and Environmental Sciences and Birmingham, Institute of Forest Research, The University of Birmingham, Edgbaston, Birmingham B15 2TT, UK*

[3]*School of Earth Sciences, Life Sciences Building, University of Bristol, Bristol, BS8 1TQ, UK*

[4]*School of Earth Sciences, Jilin University, Changchun 130061, China*

[5]*Departamento de Xeociencias Mariñas e Ordenación do Territorio, Facultade de Ciencias do Mar, Universidade de Vigo, Vigo 36310, Spain*

[6]*School of Earth and Environment, University of Leeds, Leeds LS2 9JT, UK*

[7]*Shanxi Institute of Geological Survey CO., LTD., Taiyuan 03006, China*

ABSTRACT

The global pattern of plant evolution through the Permian–Triassic mass extinction is uncertain, and the extent to which land plants were affected is debated. Detailed studies undertaken at a regional scale can help evaluate this floral transition, and thus we provide a detailed account of floral evolution from the Permian to Middle Triassic of North China based on new paleobotanical data and a refined biostratigraphy. Five floral transition events are identified from before, during, and after the Permian–Triassic crisis, including the disappearance of the gigantopterid flora (associated with loss of coal deposits), the end-Permian mass extinction of Paleophytic taxa, and gradual recovery in the Triassic with the stepwise appearance of the Mesophytic vegetation. The record begins with a Cisuralian gigantopterid-dominated rainforest community, and then a Lopingian walchian Voltziales conifer-ginkgophyte community that evolved into a voltzialean conifer-pteridosperm forest community. The last is associated with a change amongst terrestrial vertebrates from the Jiyuan fauna to a pareiasaur-dominated fauna, found in red beds that lack coal deposits due to arid conditions. The disappearance of the voltzialean conifer forest community may represent the end-Permian mass extinction of plants although it could also be a consequence of the non-preservation of plants in sedimentary red-beds. The first post-crisis plants are an Induan herbaceous lycopsid community, succeeded by the *Pleuromeia-Neocalamites* shrub marsh community. A pteridosperm shrub woodland community dominated for a short time in the late Early Triassic along with the reappearance of insect herbivory. Finally, in the Middle Triassic, gymnosperm forest communities gradually rose to dominance in both uplands and lowlands along with other diverse plant communities, indicating the establishment of the Mesophytic Flora.

INTRODUCTION

The response of plant communities to the Permian–Triassic mass extinctions is much debated (e.g., Cascales-Miñana et al., 2016; Nowak et al., 2019). There is no doubt that global floras changed substantially during the Permian–Triassic transition, from the Paleophytic Flora of the late Paleozoic to the Mesophytic Flora of the Mesozoic (Niklas et al., 1983; Cleal and Cascales-Miñana, 2014), but details of the timing are uncertain because of the absence of a robust stratigraphic framework in many terrestrial sections. Regional-scale paleobotanical and palynological work has suggested variable responses to the crisis. Palynological data from East Greenland initially suggested a significant change amongst land plants, especially the disappearance of conifers, followed by delayed recovery (Looy et al., 1999, 2001). Other studies have suggested that there is no extinction in palynological records around the Permian–Triassic boundary (Hochuli et al., 2016; Schneebeli-Hermann et al., 2017). In Australia and South Africa, a clear extinction is marked by the disappearance of the *Glossopteris* flora (Fielding et al., 2019; Vajda et al., 2020; Mays et al., 2020; Gastaldo et al., 2020; McLoughlin et al., 2021). Data from South China show a considerable loss of land plants during the Permian–Triassic mass extinction (Xiong and Wang, 2011; Yu et al., 2015; Feng et al., 2020; Broutin et al., 2020; Chu et al., 2020). The changes of macro-plant fossil assemblages from the Permian to Triassic of North China is clear (Wang, 1993, 2010; Stevens et al., 2011; Lu et al., 2020; Broutin et al., 2020) but its link with the crisis is uncertain.

The Permian–Triassic mass extinction (252 Ma) was the most severe biotic crisis in the Phanerozoic, and was associated with highly stressed conditions due to a combination of proposed factors such as global warming (Sun et al., 2012; Benton, 2018; Frank et al., 2021), acid rain (Sephton et al., 2015), wildfires (Shen et al., 2011; Chu et al., 2020), increased UV-B flux (Visscher et al., 2004; Foster and Afonin, 2005), atmospheric heavy metal pollution (Hochuli et al., 2017), increase of continental weathering (Song et al., 2015; Lu et al., 2020), and strong volcanic activity (Wignall, 2015; Benton, 2018). The crisis eliminated over 80% of marine species, 70% of terrestrial vertebrate species, and more than 50% of plant genera,

†Corresponding authors: jntong@cug.edu.cn; yujianxin@cug.edu.cn.

GSA Bulletin;
published online 14 December 2022

https://doi.org/10.1130/B36316.1; 13 figures; 1 table; 1 supplemental file.

For permission to copy, contact editing@geosociety.org
© 2022 Geological Society of America

Downloaded from http://pubs.geoscienceworld.org/gsa/gsabulletin/article-pdf/doi/10.1130/B36316.1/5749686/b36316.pdf
by University of Bristol user

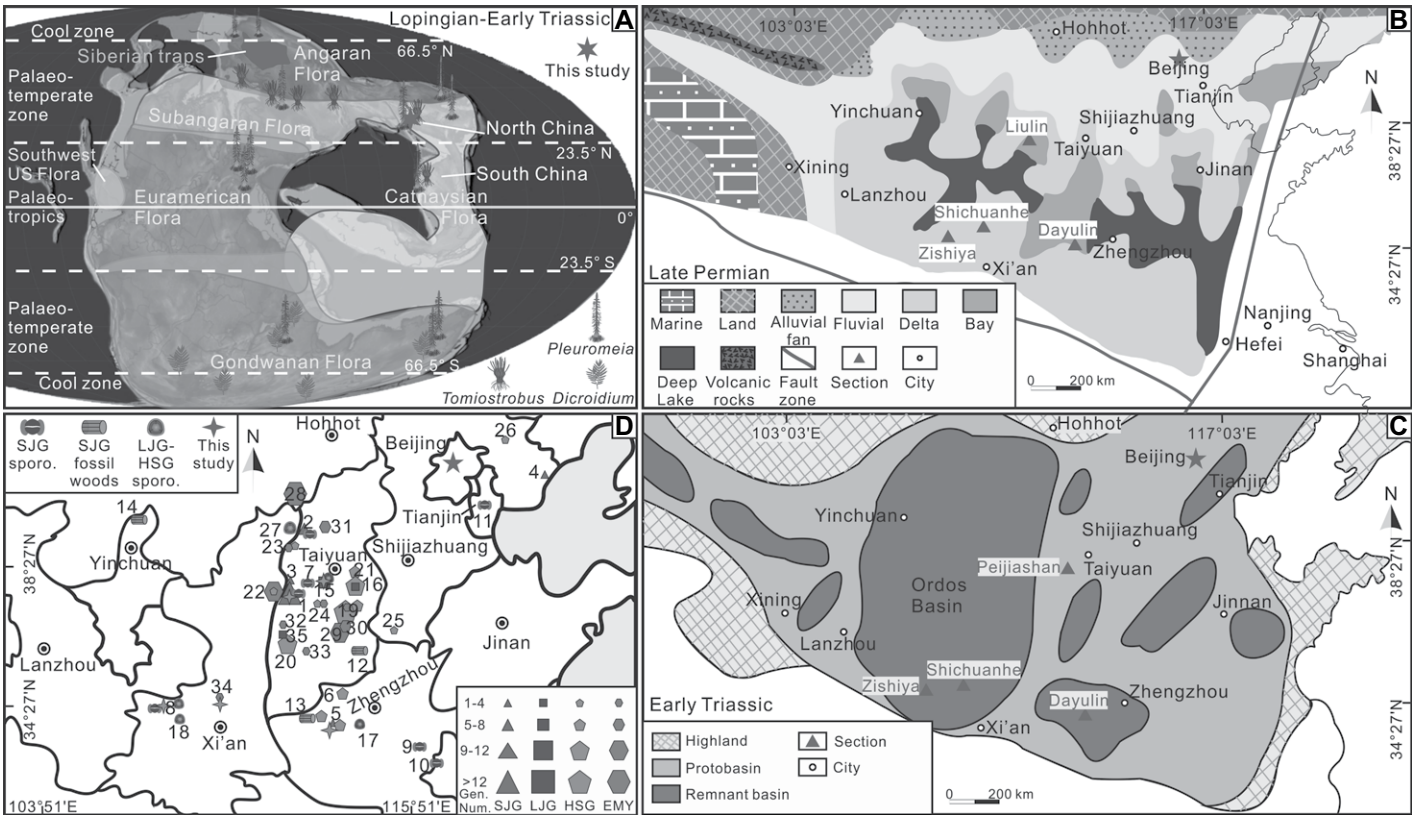

Figure 1. (A) Late Permian paleophytogeographical map and distribution of typical Early Triassic fossil plant taxa during the Late Permian to Early Triassic (Broutin et al., 1995; McLoughlin, 2001, 2011); base map adapted from Scotese (2021). (B) Paleogeographic map of the Late Permian and main sections of this study in North China; base map modified from Zhu et al. (2007). (C) Paleogeographic map of the Early Triassic and main sections of this study in North China; base map modified from Liu et al. (2015). (D) Geographic distributions of fossil plant locations from the Sunjiagou (SJG), Liujiagou (LJG), Heshanggou (HSG), and Ermaying (EMY) formations in North China (Supplemental Data File 1; see footnote 1). sporo.—sporomorphs; Gen. Num.—the number of genera.

including 42% of lycophytes and ferns and 70% of gymnosperms, and was followed by the Early Triassic coal gap (Niklas et al., 1983; Retallack et al., 1996; Rees, 2002; Benton and Newell, 2014; Cascales-Miñana et al., 2016; Stanley, 2016; Dal Corso et al., 2022).

Here we present an investigation of some groups of continental organisms using a recently refined age model for the Permian to Middle Triassic in North China. Five successive floras are established in association with corresponding vertebrate and invertebrate faunas, which record substantial changes in continental ecosystems during the Paleophytic-Mesophytic transition.

GEOLOGICAL SETTING

During the Permian, six paleofloras were developed in different paleophytogeographical provinces (Chaloner and Lacey, 1973; McLoughlin, 2001, 2011), but during the Early Triassic, provincialism was reduced and a more cosmopolitan lycopsid flora occurred over most of the Northern Hemisphere, while *Dicroidium* forests and locally abundant isoetalean and pleuromeian lycopsids covered the Southern Hemisphere (Fig. 1A). North China, with its Permian Cathaysian Flora, traversed low latitudes (~30°N), drifting north toward the north-eastern part of the Paleo-Tethys Ocean during the late Paleozoic and early Mesozoic (Fig. 1A; Wang et al., 1998). Sedimentary sequences suggest there was a large lake, ~1400 km wide, in North China during the Permian–Triassic (Figs. 1B and 1C; Zhu et al., 2007; Liu et al., 2015; Ji et al., 2021, 2022).

The Permian to Middle Triassic succession in North China is divided into the Upper Shihhotse, Sunjiagou, Liujiagou, Heshanggou, and Ermaying formations. The Upper Shihhotse Formation is dominated by grayish yellow/green sandstone with varicolored (dark red dominated) mud-siltstone. The Sunjiagou Formation comprises red thin- to medium-bedded mudstones with some red sandstones and interbedded calcareous nodules; the overall association is interpreted as a fluvial and floodplain system (Zhu et al., 2007, 2020; Ji et al., 2022). Intermittent marine flooding occurred, indicated by some marine fossils in the upper part of the formation in the southwestern part of the study region (Yin and Lin, 1979; Chu et al., 2019). The overlying Liujiagou Formation is composed of massive red sandstones with a few interbedded mud-siltstones, locally bearing wrinkle structures, usually taken as evidence of microbial mats (Chu et al., 2015; Tu et al., 2016). There are mud cracks and ripple marks in the lower part, and some large sand sheets interbedded with thick conglomerates in the middle-upper part. This unit was deposited in various fluvial or lake-shore environments (Zhu et al., 2020; Ji et al., 2022). The Heshanggou Formation consists of red siltstones interbedded with some thin sandstone beds and abundant calcareous nodules, interpreted to have formed in shallow lakes (Hu et al., 2009). The Ermaying Formation comprises grayish green, thick-bedded sandstones with green and red thin-bedded mudstones and was deposited in fluvial-lacustrine settings. Abundant fossil plants and sporomorphs have been identified

Downloaded from http://pubs.geoscienceworld.org/gsa/gsabulletin/article-pdf/doi/10.1130/B36316.1/5749686/b36316.pdf
by University of Bristol user

from various locations (Fig. 1D; Supplemental Data File 1[1]).

The ages of the studied formations have been discussed for a long time, and are derived from isolated fossils, magnetostratigraphy, chemostratigraphy, and a few U-Pb dates from ash beds. A recent U-Pb zircon study (Wu et al., 2021) shows that most of the Upper Shihhotse Formation is of latest Asselian to early Kungurian age (294.8 ± 1.2 to ≤280.73 ± 0.12 Ma) rather than Guadalupian–early Lopingian as previously thought, although its uppermost part may still be latest Capitanian–Lopingian (≤261.75 ± 0.29 Ma). Most of the Guadalupian seems to be absent in parts of North China in this new dating scheme (Wu et al., 2021) while the magnetostratigraphy of the uppermost Upper Shihhotse Formation indicates a Wuchiapingian age (Guo, 2022). The negative carbon isotope excursions in organic matter ($\delta^{13}C_{org}$) in the middle part of the Sunjiagou Formation provides a potential marker for a latest Changhsingian age (Wu et al., 2020) and a mixed marine-continental fauna marking the Permian–Triassic transitional beds was identified in the middle-upper part of the Sunjiagou Formation (Chu et al., 2019). A chemical abrasion–isotope dilution–thermal ionization mass spectrometry (CA-ID-TIMS) U-Pb age of 252.21 ± 0.15 Ma from the middle part of the Sunjiagou Formation in the Shichuanhe section also suggests a latest Changhsingian age for the middle part of the Sunjiagou Formation (Guo et al., 2022). Thus, the Permian–Triassic boundary (PTB) lies in the upper part of the Sunjiagou Formation according to carbon isotope stratigraphy, biostratigraphy, and magnetostratigraphy (Chu et al., 2019; Shu et al., 2018; Guo et al., 2019; Wu et al., 2020; Lu et al., 2020; Guo et al., 2022). The basal beds of the overlying Liujiagou Formation yield the *Aratrisporites-Alisporites* sporomorph assemblage (Ouyang and Zhang, 1982; Ouyang and Wang, 1985), and the lycopsid *Pleuromeia* occurs in the upper part of the Liujiagou Formation (Wang and Wang, 1982), all indicating an Early Triassic age (Wang, 1993; Shu et al., 2018; Guo et al., 2019), as does a laser ablation–inductively coupled plasma–mass spectrometry age of 251 ± 4 Ma from the middle part of the Liujiagou Formation (Zhu et al., 2019). Magnetostratigraphy suggests the Induan–Olenekian boundary is found in the lower part of the Liujiagou Formation (Guo et al., 2022). The Heshanggou Formation yields abundant trace fossils together with body fossils (e.g., fossil plants, vertebrates, fishes, conchostracans (= diplostracans), and ostracodes) of late Early Triassic age (Wang et al., 1978; Qu et al., 1983; Nesbitt et al., 2011). Moreover, magnetostratigraphy confirms an Olenekian age for the Heshanggou Formation (Guo et al., 2022). An ID-TIMS U-Pb zircon date of 243.528 ± 0.069 Ma dates the upper member of the Ermaying Formation as Anisian (Middle Triassic) (Liu et al., 2018). Magnetostratigraphy indicates the Olenekian–Anisian boundary occurs in the basal Ermaying Formation (Guo et al., 2022).

Here, we focus on five Permian–Triassic sections that yield well-preserved fossil plants: the Liulin, Peijiashan, Dayulin, Shichuanhe, and Zishiya sections (Figs. 1B, 1C, and 2). In addition, we also mention some other fossil sites with rich plant fossils, such as Heshun, Pingyao, and Yushe in Shanxi Province, China. In the following account, we first focus on the biotas. The potential taphonomic issues that might bias the results will be detailed in the discussion.

MATERIALS AND METHODS

This study is mainly based upon over 1400 plant megafossil specimens collected from eight locations ranging through all the target formations in North China (Table 1). These include compression, impression, and permineralized fossils. The fossils represent shoots, leaves, cones, or fertile parts and some trunks/fossil woods, most of which were identifiable. We also restudied all reported fossils from North China and in total we note 52 genera of vertebrates, 42 genera of invertebrates, 102 genera, and some form types of plants from over 120 locations (Supplemental Data Files 1–7; see footnote 1). In addition, some well-preserved cuticles were prepared by HF/HCl maceration and Schultze solution for oxidation, and KOH to remove remnant humic acids (Kerp, 1990; Jones and Rowe, 1999). In situ pollen from male cones or fertile shoots were processed by HF/HCl maceration (Jones and Rowe, 1999). All fossils studied are stored in the paleontological collection of the State Key Laboratory of Biogeology and Environmental Geology, China University of Geosciences (Wuhan, China).

Plant megafossil specimens were photographed using a Canon EOS 7D digital camera, and some in situ pollen, bract-scale complexes, small shoots and conchostracan specimens were examined and photographed using a LEICA-DM-750P microscope equipped with an automatic camera image stacking system. Some photos were processed by focus stacking methods using Photoshop CS5 (auto-align layers and auto-blend layers). Some in situ pollen were studied using a Hitachi SU8010 scanning electron microscope. In addition, one tetrapod tooth fossil from the uppermost Upper Shihhotse Formation and one well-preserved strobilus of *Pleuromeia* from the Liujiagou Formation were scanned using a nanoVoxel 4000 micro-computed tomography scanner (Sanying Precision Instruments, Tianjing, China) and the raw projections were converted into image stacks using VoxelStudio Recon (Sanying Precision Instruments). The isometric voxel size (spatial resolution) for the *Pleuromeia* and the tooth were 31.60 μm and 17.63 μm, respectively. To image the inner structure of the tooth, its volume data were segmented using the watershed algorithm in Avizo 8.0, and manual correction was performed to correct defects.

For paleoecological analysis, we normalized genera of fossil plants as binary data, present (1) or absent (0), in each formation (Cleal et al., 2021). The presence-absence matrix was then analyzed in R by hierarchical clustering using the Euclidean complete method, *k*-means clustering and principal components analysis (Figs. S3–S5; see footnote 1 for all Supplemental figures and data files). The R code is provided in the Supplemental material. To calculate the hygrophyte(H)/xerophyte(X) ratio, plant genera were classified as hygrophytes, mesophytes, and xerophytes based on previous studies (Supplemental Data Files 9 and 10) and then the ratio calculated as $[H/(H + X)]/[X/(H + X)]$ (DiMichele et al., 2020; Koll and DiMichele, 2021; Supplemental Data File 10).

MACROFLORAS FROM PERMIAN TO MIDDLE TRIASSIC IN NORTH CHINA

Based on collected specimens and previously reported data, five successive macrofloras were identified from the Permian to Lower Triassic in North China. Previously, most of the floras were named after the formations in which they occurred, but here we consistently refer to them based on the index fossils because some of the floras span more than one formation. The gigantopterid flora in the Upper Shihhotse

[1]Supplemental Material. Description of studied sections, biostratigraphy of Lopingian–Middle Triassic in North China, the results of statistical analysis, R scripts, and Supplemental Data Files: (1) Geological distributions of fossil plants, sporomorphs and fossil woods; (2) Detailed descriptions of floras in North China; (3) Plant genera distributions and number of genera in each stratigraphic unit; (4) Plant zones, subzones and assemblages from Cisuralian to Anisian in North China; (5) Invertebrate genera distributions and number of genera in each stratigraphic unit; (6) Insect genera distributions and number of genera in each stratigraphic unit; (7) Vertebrate genera distributions and number of genera in each stratigraphic unit; (8) Global floral changes from Lopingian to Middle Triassic; (9) Hygrophyte, mesophytes and xerophyte element distributions; (10) Hygrophte and Xerophyte ratios. Please visit https://doi.org/10.1130/GSAB.S.21091498 to access the supplemental material, and contact editing@geosociety.org with any questions.

Downloaded from http://pubs.geoscienceworld.org/gsa/gsabulletin/article-pdf/doi/10.1130/B36316.1/5749686/b36316.pdf
by University of Bristol user

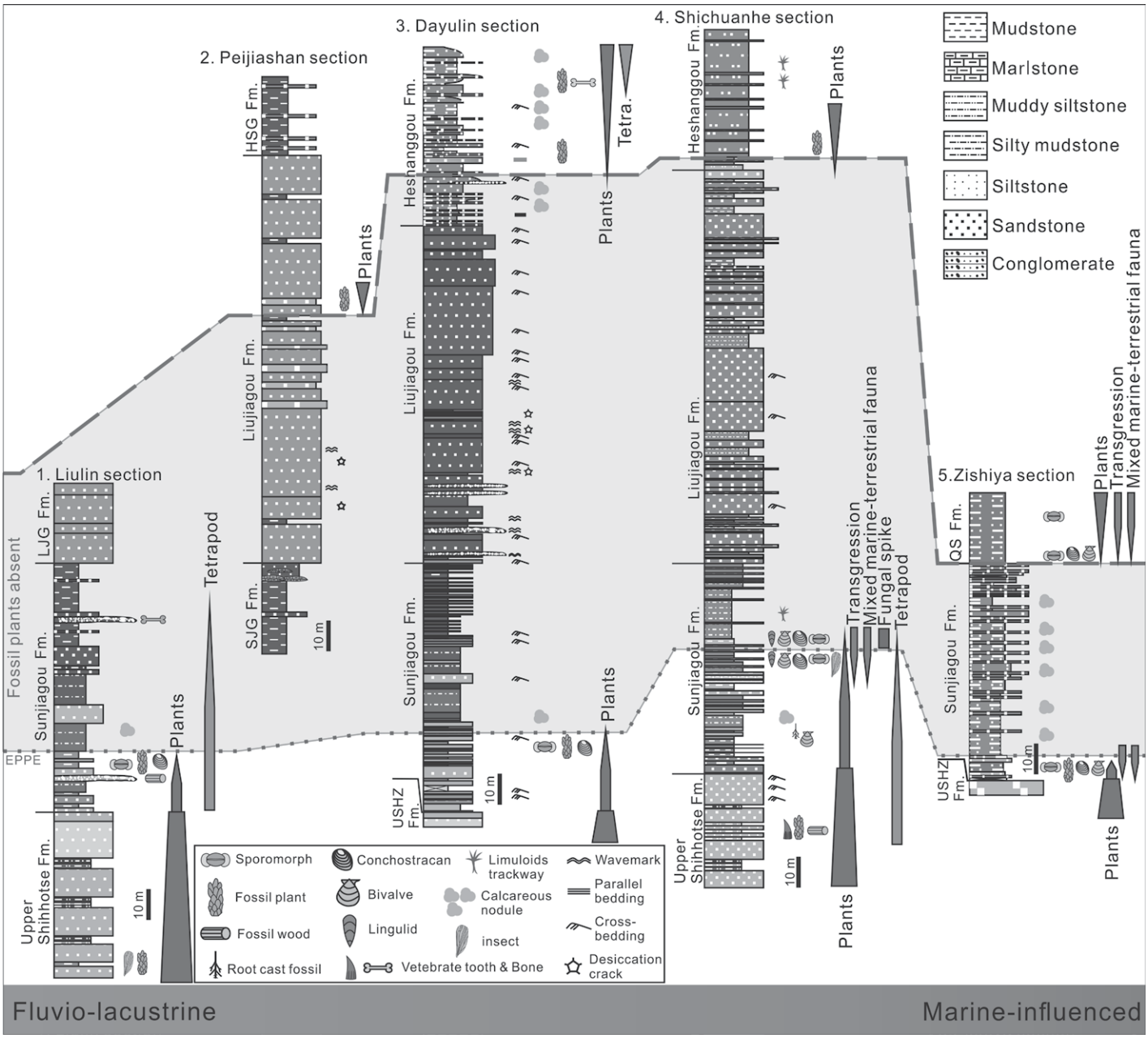

Figure 2. Lithological columns of the studied sections in North China showing the lithology and the position of the fossil horizons and some special sedimentary structures. Lower dotted line marks the end-Permian plant extinction event (EPPE), the gray area indicates the ecological disturbance interval without fossil plants, and the upper dashed line marks the occurrence of Early Triassic fossil plants in the studied sections. Fm.—Formation; Tetra.—Tetrapods; LJG—Liujiagou Formation; SJG—Sunjiagou Formation; HSG—Heshanggou Formation; USHZ—Upper Shihhotse Formation; QS—Qishan Formation.

TABLE 1. THE NUMBER OF SPECIMENS OF MACROFOSSIL PLANTS FROM DIFFERENT FORMATIONS AND SECTIONS OF NORTH CHINA IN THIS STUDY

	Liulin Section	Peijiashan Section	Dayulin Section	Shichuanhe Section	Zishiya Section	Heshun Section	Yushe Section	Pingyao Section	T.
HSG Fm.							280	120	400
LJG Fm.		80		10		10			100
SJG Fm.	206		37		202				445
USH Fm.	46			385					432
T.	252	80	37	395	202	10	280	120	1337

Notes: USH Fm.—Upper Shihhotse Formation; SJG Fm.—Sunjiagou Formation; LJG Fm.—Liujiagou Formation; HSG Fm.—Heshanggou Formation; T.—total specimens.

Formation has been well-studied previously (Wang, 2010; Stevens et al., 2011) and we confirm those earlier results. Here we focus on the other four macrofloras, i.e., the Voltziales flora in the uppermost part of the Upper Shihhotse and the Sunjiagou formations, the *Pleuromeia-Neocalamites* flora in the middle-upper part of the Liujiagou and the base of the Heshanggou formations, the *Pleuromeia-Tongchuanophyllum*

Downloaded from http://pubs.geoscienceworld.org/gsa/gsabulletin/article-pdf/doi/10.1130/B36316.1/5749686/b36316.pdf
by University of Bristol user

flora in the lower-upper part of the Heshanggou and the basal part of the Ermaying formations, and the *Lepacyclotes-Voltzia* flora in the lower to upper parts of the Ermaying Formation.

The Voltziales Flora

This flora occurs in the uppermost part of the Upper Shihhotse Formation and the lower part of the Sunjiagou Formation. It is dominated by Voltziales conifers, including walchian and voltzian voltzialean type conifers. Here the Voltziales flora is subdivided into the ginkgophyte–walchian Voltziales and the voltzian Voltziales subfloras.

The Ginkgophyte–Walchian Voltziales Subflora

This subflora occurs in the uppermost part of the Upper Shihhotse Formation of the Liulin (Fig. 2; Fig. S1B) and Shichuanhe sections (Fig. 2; Fig. S1C). It is dominated by walchian voltzialean shoots, other vegetative-shoot types of conifers (form type 0, 2, and 5, in Supplemental Data File 2), and includes ginkgophytes (form type 1 and 2, in Supplemental Data File 2), pteridosperms (*Autunia*), putative cycadophytes (*Taeniopteris*), and *Sphenopteris*-type foliage (Fig. 3). Gymnosperms are the main elements in this subflora. In the uppermost Upper Shihhotse Formation of the Liulin section, over 80% of plant fossils are shoots and leaves, whereas seed fossils account for ~20%. Around 85% of the shoot compressions/impressions are assigned to conifers and most of these conifer shoots are walchian Voltziales according to their gross morphology and cuticles (Fig. 3, description in Supplemental Data File 2). Some ginkgophyte leaves and *Taeniopteris* locally co-occur with the conifer shoots. In the uppermost Upper Shihhotse Formation of the Shichuanhe section, 385 specimens were collected and 256 identified. Among these, over 65% are assigned to conifer shoots, ~25% are ginkgophyte leaves, and there are a few *Autunia*-type pteridosperm ovuliferous organs, noeggerathialean leaves, and other foliage types. In addition, there are some in situ monosaccate pollen associated with walchian voltzialean shoots that are elliptical to circular in polar view (Figs. 3X and 3Y), showing a monolete suture on the corpus, a punctate or in some cases a rugulate surface. These are assigned to *Potonieisporites*. This subflora is named the ginkgophyte–walchian Voltziales subflora, after its two dominant elements.

The Voltzian Voltziales Subflora

This subflora of the Voltziales flora was identified from the lower part of the Sunjiagou Formation in the Liulin (Fig. 2; Fig. S1E), Dayulin (Fig. 2; Fig. S1F), and Zishiya (Fig. 2; Fig. S1G) sections. It is dominated by conifers, including *Pseudovoltzia*-type/*Ullmannia*-type and other undefined vegetative shoots with well-preserved cuticles (form type 1–4, description in Supplemental Data File 2), *Pseudovoltzia*-type bract-scale complexes with five-lobed scales (Fig. 4AA), male cones with in situ monolete bisaccate pollen of the *Gardenasporites*-type (Figs. 4DD, 4EE, 4PP, and 4SS) and seeds, with some pteridosperms, such as *Autunia*-type peltate ovuliferous organs, and *Germaropteris*-type vegetative small leaves with well-preserved cuticles (Fig. 4, description in Supplemental Data File 2). *Calamite* stems occur sporadically as compressions or impressions. In the lower part of the Sunjiagou Formation of the Liulin section, 220 discernible specimens were found, 76% of which are shoots, 11% seeds, and 13% fertile parts. Around 96% of the shoot compressions/impressions can be assigned to conifers and 4% to ferns and pteridosperms. In the lower part of the Sunjiagou Formation of the Dayulin section, 37 identifiable specimens were collected, all of which are conifer shoot compressions and isolated conifer leaf compressions. In addition, there are over 300 specimens from the lower part of the Sunjiagou Formation of the Zishiya section and 202 of these were identifiable. Of these, shoots comprise ~70%, seeds around 19%, fertile parts (including cones) ~8%, and a few stems ~3%. All shoots and one cone can be assigned to conifers, the other fertile parts to the *Autunia* type, a few stems to *Calamites*, and some dispersed seeds to conifers or pteridosperms. This subflora is named after the dominant element of the conifer as the voltzian Voltziales subflora.

The Pleuromeia-Neocalamites Flora

Only a few localities, such as Jiaocheng, Yushe, and Heshun in Shanxi, yield these plant fossils. They come from the middle-upper part of the Liujiagou Formation and the base of the Heshanggou Formation (Fig. 2). Most of these plant fossils are strobili, isolated sporophylls, and rhizomorphs of *Pleuromeia jiaochengensis* and *Pleuromeia sternbergii* (Figs. 5C–5K and 6A–6D, and 6M). Numerous fragments of in situ stems of *Neocalamites* or *Equisetites* preserved as compressions or casts also occur in both red silty mudstones and gray-green siltstones (Figs. 6E–6K). Fragments of strap-shaped leaves with parallel veins are possible gymnosperms. Some fragments of sporophylls with long tips characteristic of *Tomiostrobus* were found at the base of the Heshanggou Formation at Heshun (Fig. 6L). In addition, some broken fronds of *Scolopendrites* (Figs. 5A and 5B) and some dispersed possible male cones, bract-scale complexes and seeds of voltzialean conifers (Figs. 6N–6O) occur in this flora. Potential cycadophytes are identified as *Taeniopteris*. This flora is named after the two dominant elements, *Pleuromeia* and *Neocalamites*. *Pleuromeia* by itself is not diagnostic of an individual flora as its stratigraphic range extends into the overlying *Pleuromeia-Tongchuanophyllum* and *Lepacyclotes-Voltzia* floras (see below).

The Pleuromeia-Tongchuanophyllum Flora

Abundant fossil plant specimens occur in the lower-upper part of the Heshanggou Formation and the basal part of the Ermaying Formation in the Yushe, Pingyao, and Puxian sections in Shanxi. Numerous plant fossils have been previously reported from this interval from many other localities, such as Shouyang, Pingyao, Puxian, Fengfeng, Chengde, Jiyuan, and Yima (Supplemental Data Files 2 and 3). Most of them are lycophytes, e.g., *Pleuromeia epicharis*, some stems with very small leaf cushions *Mesolepidodendron*, some sporophylls with long tips of *Tomiostrobus* (Figs. 7A–7D, 7G, 7H, and 7J–7L), and pteridosperms (up to nine genera, e.g., *Tongchuanophyllum*, *Neoglossopteris*, "*Gangamopteris,*" *Glossophyllum*, "*Euryphyllum,*" *Scytophyllum*, "*Thinnfeldia,*" *Sphenopteris,* and *Peltaspermum*) (Figs. 7M–7O), and the others are sphenophytes (e.g., *Neolobatannularia*, *Phyllotheca*, *Neocalamites*, *Equisetites*) (Figs. 7I), pteridophytes (e.g., *Anomopteris, Scolopendrites, Neuropteridium, Todites*), conifers (*Voltzia*, *Yuccites*, *Willsiostrobus*) (Figs. 7P and 7Q), and putative cycadophytes (possibly *Cycadocarpidium*) (Supplemental Data Files 2 and 3). This flora is named after its abundant lycopods, dominated by *Pleuromeia*, and the common occurrence of *Tongchuanophyllum*.

The Lepacyclotes-Voltzia Flora

This flora occurs in the lower to upper parts of the Ermaying Formation where the Mesophytic floral elements gradually appear and become more diverse. However, some lycophyte rhizophores (*Pleuromeia*), some lycophyte sporophylls with short tips (*Lepacyclotes*), *Isoetites*, and sphenophytes (*Neocalamites* and *Equisetites*) remain common but sphenophyte stems became larger than those in the former floras (Fig. 8). Fronds and pinnules of true ferns from the lower to upper parts of the Ermaying Formation were identified as *Anomopteris*, *Cladophlebis*, *Danaeopsis*, *Symopteris* (*Bernoullia*), and *Todites* (Supplemental Data Files 2 and 3). In addition, there is a

Downloaded from http://pubs.geoscienceworld.org/gsa/gsabulletin/article-pdf/doi/10.1130/B36316.1/5749686/b36316.pdf
by University of Bristol user

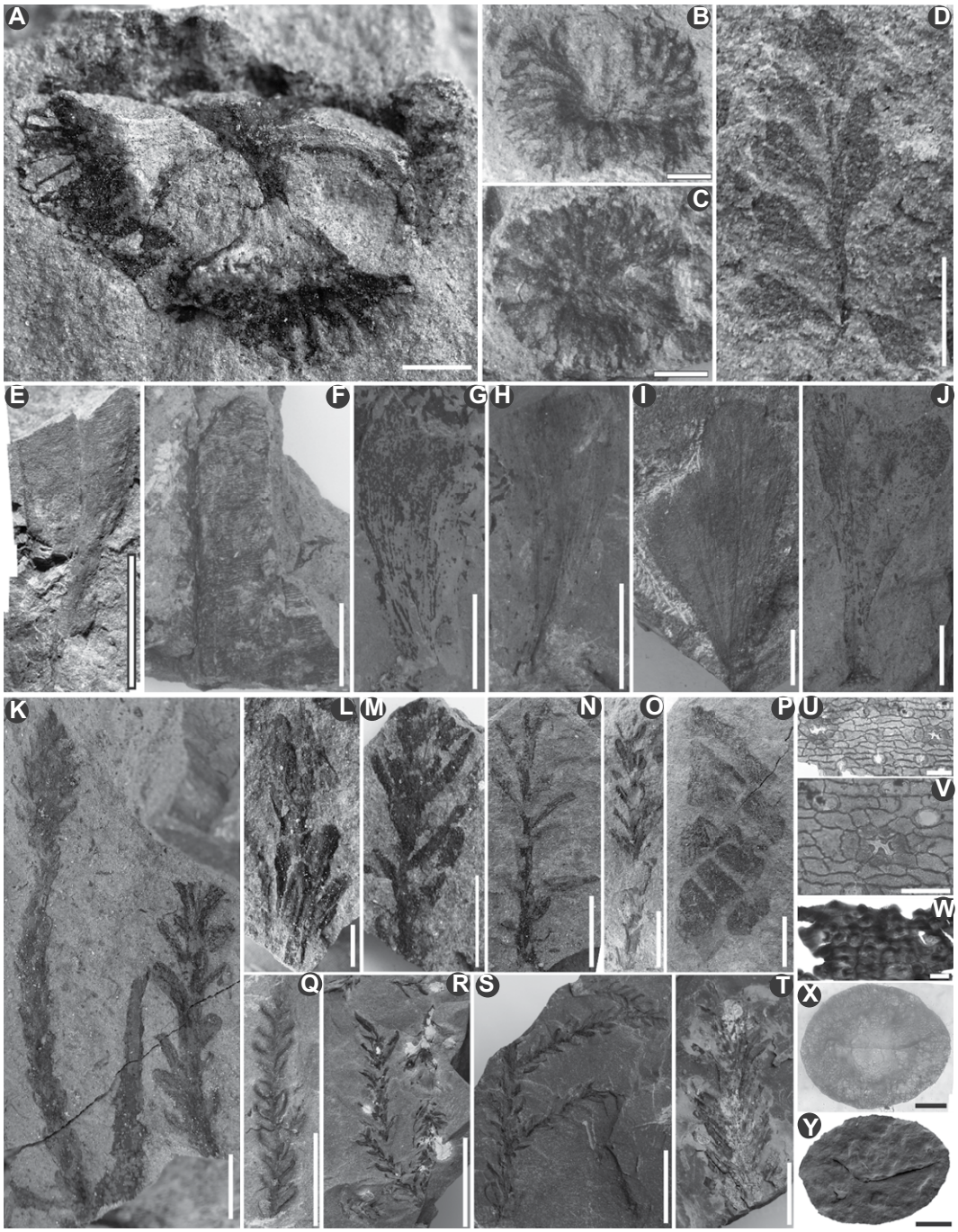

Figure 3. Plant fossils, cuticles, and in situ pollens from the top part of the Upper Shihhotse Formation of the Shichuanhe and Liulin sections in North China. (A–C) *Autunia*-type ovuliferous organs. (D) Small fragmentary pinna of *Sphenopteris*. (E and F) Strap-like leaf in E and broken leaf in F of *Taeniopteris* with simple parallel lateral veins arising from the midvein at an angle of nearly 90°. (G–J) Broken leaves of ginkgophytes, G and H, broken leaves of ginkgophyte type 2 with horn-like shape and dichotomous-patterned veins, I and J, broken wedged-shape leaves with the bifurcated rounded apex of ginkgophyte type 1 with strong petioles. (K–O, T, and W) shoots and cuticle of conifer type 2, K with possible terminate cone on the shoot, the cuticle in W is from the shoot in T. (P) Possible cone of a conifer. (Q–S, U, V, X, and Y) Shoots, cuticles, and in situ pollens of conifer type 0, U and V are cuticles macerated from the shoot in S, X, and Y are in situ pollens "picked out" directly from the shoots in Q–S and pollen in Y was photographed under scanning electron microscope. Scale bars: A–D, L, and T are 5 mm. E–K and M–S are 1 cm. U, V, X, and Y are 50 µm, W is 20 µm. A–D, F, I–J, K–O, and P are from the Shichuanhe section. E, G–H, Q–T, and Q–Y are from the Liulin section.

diverse flora of pteridosperms (e.g., *Germaropteris*, *Peltaspermum*, *Ptilozamites*, *Glossophyllum*, *Neoglossopteris*, *Scytophyllum*, *Tongchuanophyllum*, "*Thinnfeldia,*" *Pachypteris*, and *Protoblechnum*), cycadophytes (e.g., *Nilssonia*, *Sinozamites*, and *Taeniopteris*), ginkgophytes (e.g., *Baiera*, *Ginkgoites*, and *Sphenobaiera*), and conifers (e.g., *Pagiophyllum*, *Podozamites*, *Voltzia*, and *Yuccites*) (Supplemental Data Files 2 and 3). This flora is named after the common Middle Triassic elements, *Lepacyclotes* and *Voltzia*.

DISCUSSION

Ages of the Lopingian to Middle Triassic Macrofloras in North China

The floras of North China can be dated with reference to other fossils such as vertebrates. The ginkgophyte–walchian Voltziales subflora of the uppermost Upper Shihhotse Formation of the Shichuanhe and Liulin sections co-occurs with a vertebrate tooth fossil (Figs. 9A–9D) of the Jiyuan fauna (Fig. S2; Xu et al., 2015). The Jiyuan Fauna comprises abundant vertebrate taxa (Supplemental Data File 7; Xu et al., 2015) that are assigned a Wuchiapingian age based on comparisons of the entire tetrapod assemblage to the Ilinskoe Subassemblage of the Sokolki Assemblage in Russia and the *Cistecephalus* Assemblage Zone in South Africa (Liu et al., 2014; Benton 2016). A Wuchiapingian age of the strata is also supported by magnetostratigraphy (Guo, 2022).

Previously a *Ullmannia bronnii–Yuania magnifolia* assemblage was documented by

Downloaded from http://pubs.geoscienceworld.org/gsa/gsabulletin/article-pdf/doi/10.1130/B36316.1/5749686/b36316.pdf
by University of Bristol user

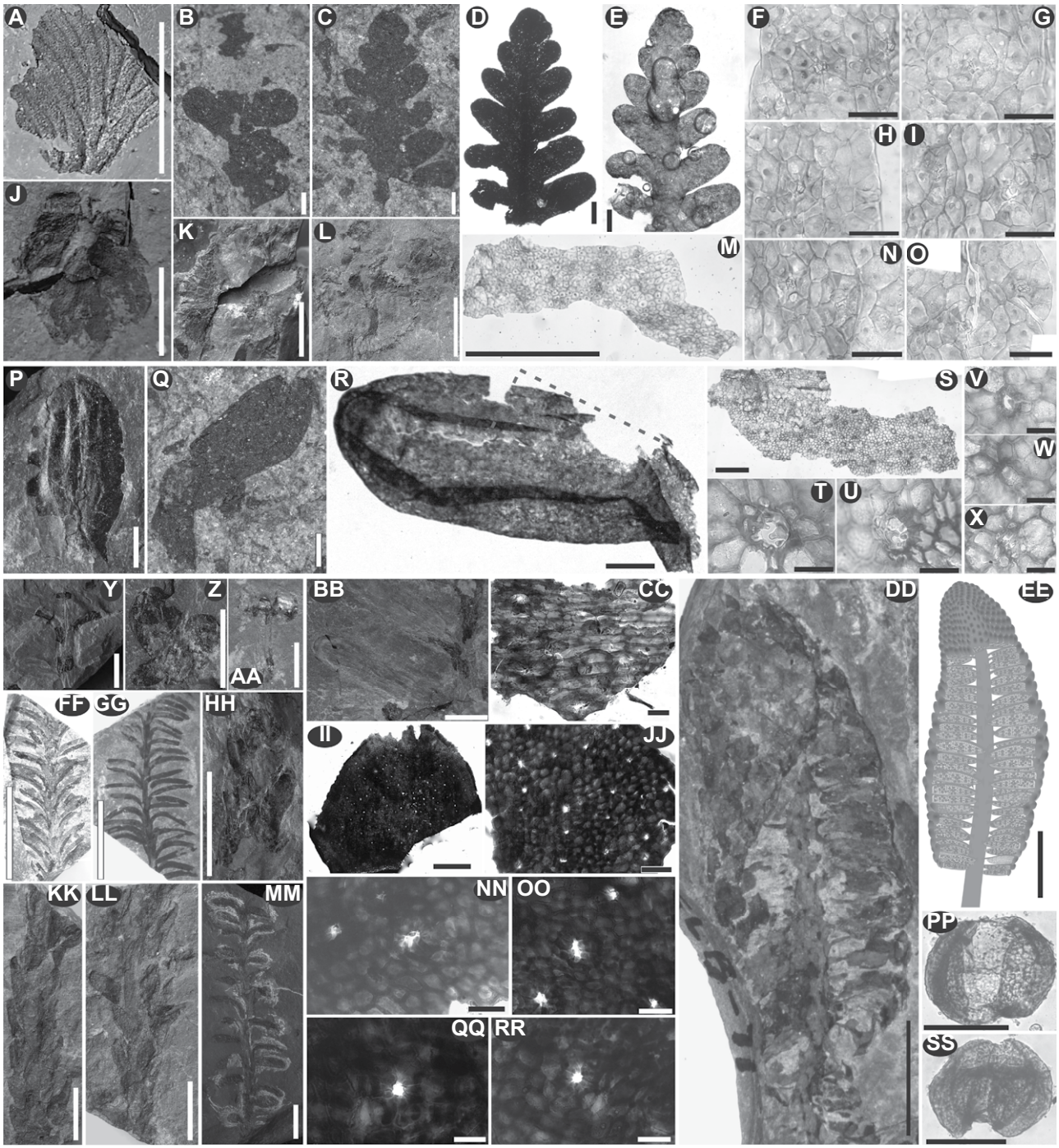

Figure 4. Plant fossils, cuticles, and in situ pollens from the lower part of the Sunjiagou Formation of the Liulin, Dayulin, and Zishiya sections in North China. (A) Fragments of pinnule of pteridophyte with dichotomous veins. (B–I and M–O) Vegetative terminal pinnae of *Germaropteris martinsii* and its cuticles, triangular arrows in N and O show the base of trichome, D before processing, E after processing, F–I and M–O are from the red rectangular area of E. (J–L) Fertile parts of the *Autunia*-type organ. (P–Y and MM) Shoots and isolated leaves of conifer type 3 of *Pseudovoltzia* with well-preserved cuticle, R–X are from Q, S–X is from the red rectangular area of R. (AA) Bract-scale complexes of fossil conifers. (BB and CC) Heterophyll shoot and its cuticles of conifer type 2. (DD, EE, PP, and SS) Male cone of conifer and its in situ pollens (possible *Gardenasporites*), EE is a reconstruction of DD, PP is the distal view, and SS is the proximal view of pollen grains. (FF and GG) Some shoots of conifer type 4. (Z, HH–LL, NN, OO, QQ, RR) Some conifer shoots with their cuticles of conifer type 1. Scale bars: A, J, Y, Z, AA, and BB are 5 mm. K, L, DD–HH, KK, LL, and MM are 1 cm. B–E and P–R are 1 mm. F–I, N–O, T–X, CC, and NN–SS are 50 µm. M, S, and II are 500 µm. JJ is 200 µm. A–J, M–O, DD–GG, PP, and SS are from the Liulin section. P–Z, AA–CC, HH–JJ, NN, OO, QQ, and RR are from the Dayulin section. K, L, and KK–MM are from the Zishiya section.

Downloaded from http://pubs.geoscienceworld.org/gsa/gsabulletin/article-pdf/doi/10.1130/B36316.1/5749686/b36316.pdf
by University of Bristol user

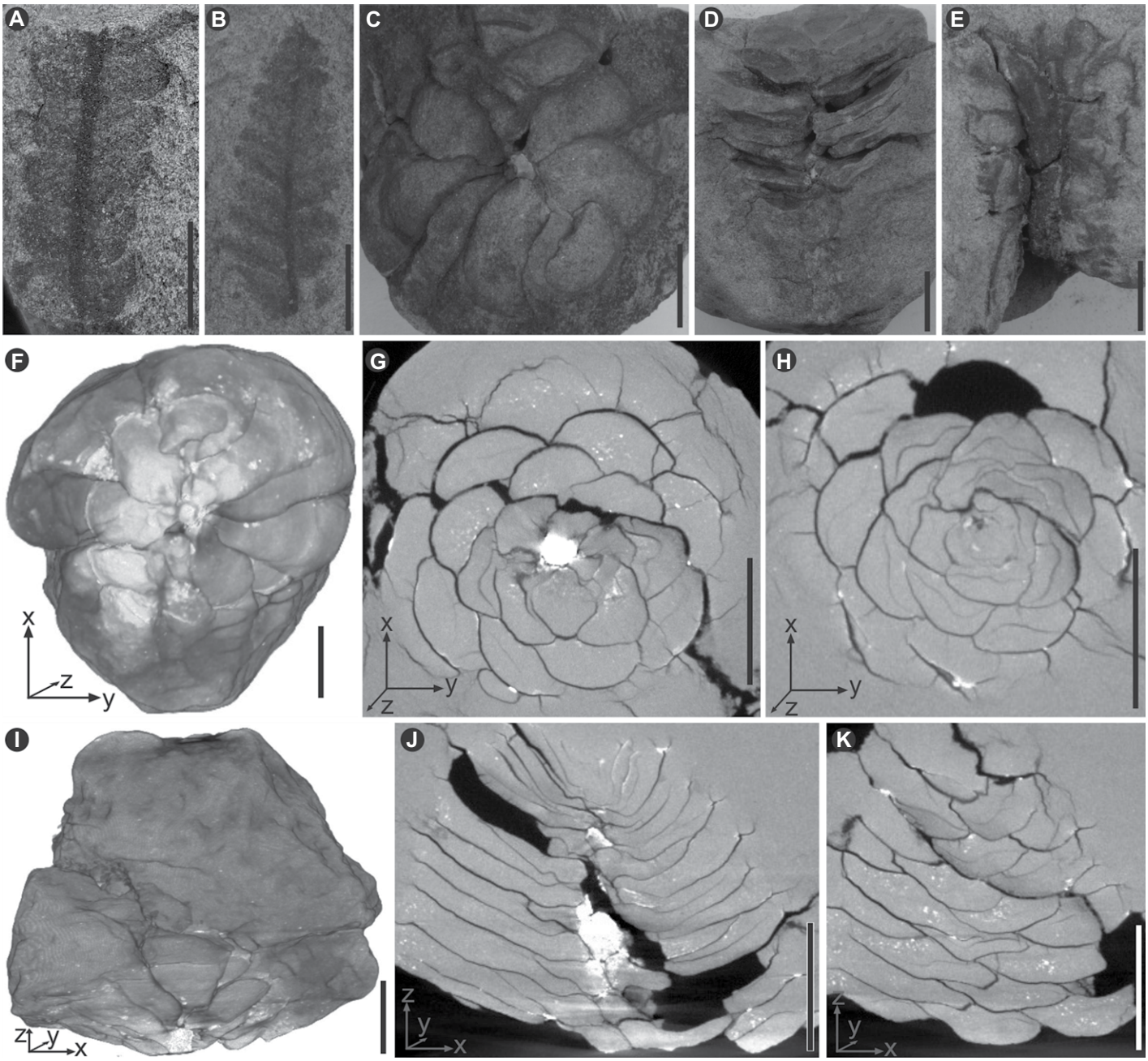

Figure 5. Strobili of *Pleuromeia* and pinnate fragments of pteridophylls from the upper part of the Liujiagou Formation of the Peijiashan section in North China. (A and B) Pinnate fragments of *Scolopendrites*. (C–K) Strobili of *Pleuromeia*. (F–K) were processed under CT scanning. All scale bars are 1 cm.

Wang and Wang (1986) from the lower-middle part of the Sunjiagou Formation of North China. Unfortunately, we have not collected any *Yuania* in these strata during our reinvestigation (Supplemental Data Files 2 and 3), thus herein we use the term *Ullmannia–Pseudovoltzia–Germaropteris* assemblage as a replacement name. The *Ullmannia–Pseudovoltzia–Germaropteris* assemblage corresponds to the voltzian Voltziales subflora. This subflora and the corresponding *Lueckisporites virkkiae–Jugasporites schaubergeroides* sporomorph assemblage (Hou and Ouyang, 2000) co-occur with a *Pseudestheria* (Figs. 9H–9K) conchostracan assemblage in the Liulin and Dayulin sections (Figs. 2 and 9; Fig. S2), which is assigned to the Lopingian (probably Changhsingian). In North China, some pareiasaurs (Wang et al., 2019) and fish fossils (Chondrostei and *Platysomus*) (Wang, 1981) were reported from the Sunjiagou Formation and the laterally equivalent Naobaogou Formation (Liu and Bever, 2018; Fig. S2; Supplemental Data File 7). In addition, the *Darwinula-Panxiania* ostracod assemblage occurs in the middle part of the Sunjiagou Formation (Chu et al., 2015; Fig. S2; Supplemental Data File 5). Further, mixed continental-marine biotas (Fig. 9), comprising conchostracans, plants, insects, marine bivalves, and lingulid brachiopods, in

Downloaded from http://pubs.geoscienceworld.org/gsa/gsabulletin/article-pdf/doi/10.1130/B36316.1/5749686/b36316.pdf
by University of Bristol user

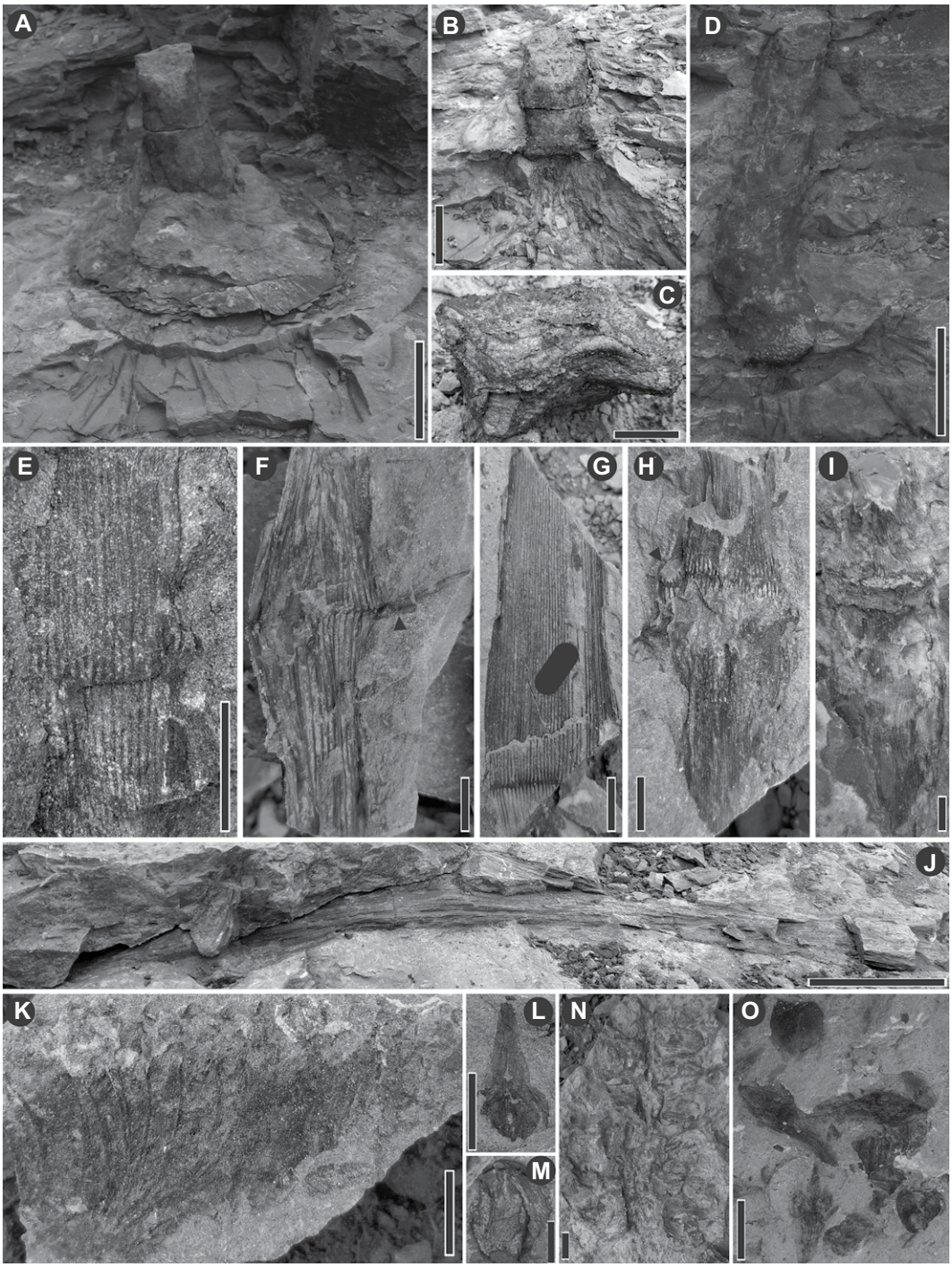

Figure 6. In situ stems/rhizomorphs and dispersed megasporophylls of *Pleuromeia*, dispersed broken megasporophylls of *Tomiostrobus*, in situ rhizomes, and dispersed stems of *Neocalamites* and *Equisetites* and isolated possible male cone, bract-scale complexes, and seeds of voltzian conifers from the basal Heshanggou Formation of the Heshun section in North China. (A–D) in situ stems/rhizomorphs of *Pleuromeia*, C is the bottom of B showing four-lobed rhizomorphs. (E–J) Some in situ rhizomes and dispersed stems of *Neocalamites*; in F the triangular arrow shows the linear whorled leaves at the node; in H the triangular arrow shows one small branch base at the node; J shows the underground part of the rhizome and the triangular arrow shows the upright stem. K shows a broken stem of *Equisetitees*. L shows a dispersed broken megasporophyll with a long tip characteristic of *Tomiostrobus*. M shows a dispersed megasporophyll of *Pleuromeia*. N shows one isolated possible male cone. O shows a bract-scale complex and cordiform seeds of voltzian conifers. Scale bars: A, B, D, and J are 5 cm; C is 2 cm; E–I and K–O are 1 cm.

the middle part of the Sunjiagou Formation are particularly important for biostratigraphic correlation between continental and marine facies (Chu et al., 2019). All the floral data suggest the Permian–Triassic transitional beds start in the middle part of the Sunjiagou Formation. This is further supported by a CA-ID-TIMS U-Pb age of 252.21 ± 0.15 Ma from the middle part of the Sunjiagou Formation in the Shichuanhe section (Guo et al., 2022).

However, some pareiasaurs were also found from the uppermost part of the Sunjiagou Formation at the Xuecun section, Liulin, Shanxi Province (Wang et al., 2019; Fig. S2; Supplemental Data File 7). Pareiasaurs from the continental sections in Russia and South Africa are not considered to have survived the Permian–Triassic mass extinction (Lee, 1997; Benton, 2016). Meanwhile, abundant microbial-induced sedimentary structures (MISS), such as wrinkle structures, appear in the top part of the Sunjiagou Formation and lower part of the Liujiagou Formation at Dayulin (Yiyang, Henan Province, China), and are common in post-extinction environments (Chu et al., 2015; Tu et al., 2016), as seen in high southern latitudes (Mays et al., 2021a, 2021b). Consequently, the age of the upper part of the Sunjiagou Formation is unclear. The uncertainty over the age of the top of the Sunjiagou Formation may be because the tran-

Downloaded from http://pubs.geoscienceworld.org/gsa/gsabulletin/article-pdf/doi/10.1130/B36316.1/5749686/b36316.pdf
by University of Bristol user

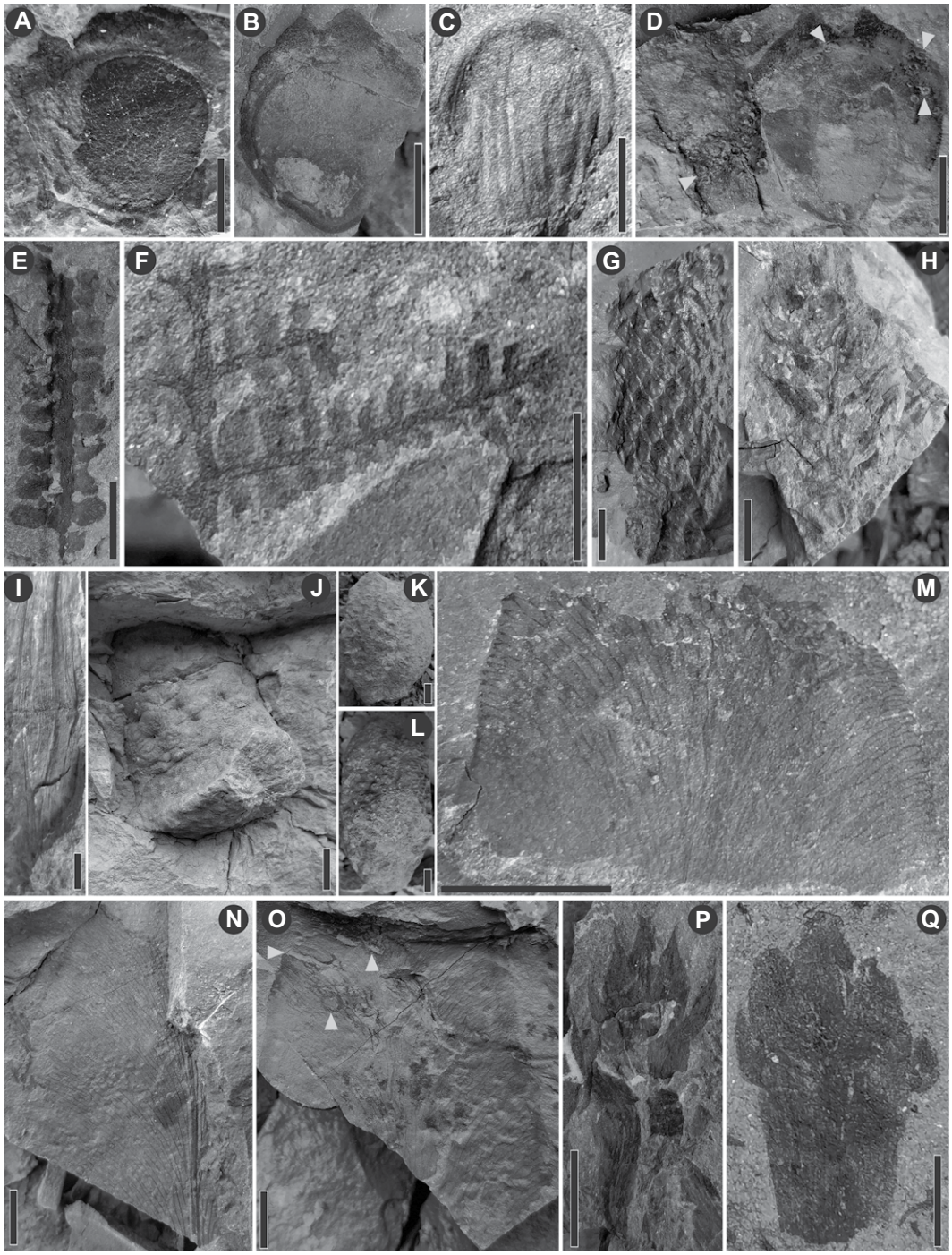

Figure 7. Plants from the Lower Heshanggou Formation of the Yushe section in North China. (A–D) Megasporophylls of *Pleuromeia*, some microconchids on the surface of D at the triangular arrows. (E and F) Pinnae of *Anomopteris*. (G) Stem of *Pleuromeia*. (H) Strobilus of *Pleuromeia*. (I) The broken stem of *Neocalamites*. (J–L) In situ rhizophores of *Pleuromeia*. (M–O) Leaves of *Tongchuanophyllum*, showing feeding holes on the surface and margins of O at the triangular arrow. (P and Q) Bract-scale complexes of voltzian conifers. Scale bars: A, C, F, and Q are 5 mm; B, D, E, and G–P are 1 cm.

sition with the overlying Liujiagou Formation is diachronous. An *Aratrisporites-Alisporites* sporomorph assemblage, in which *Aratrisporites* is the most abundant element (13.4%), and *Alisporites* is a sub-dominated element (10.3%), occurs with a few fragmentary fossils of *Dicynodon* in the lower part of the Liujiagou Formation (Ouyang and Zhang, 1982; Fig. S2; Supplemental Data File 7), indicating an earliest Triassic (Induan) age. This conclusion is further supported by magnetostratigraphy that indicates a likely Dienerian age for this level (Guo et al., 2022).

In the middle part of the Liujiagou Formation in the Peijiashan section and the base of the Heshanggou Formation in the Shichuanhe, Heshun, and Yushe sections, the *Pleuromeia-Neocalamites* flora co-occurs with a conchostracan *Leptolimnadia-Paleoleptestheria* assemblage and some Triopsidae (Fig. S2; Supplemental Data File 5; Tong et al., 2019). Furthermore, from the lower-middle part of the Qishan Formation (equivalent to the Liujiagou Formation) of the Zishiya section, we found a *Lundbladispora–Cycadopites–Protohaploxypinus* sporomorph assemblage that can be correlated to the *Densoisporites nejburgii–Lunatisporites–Cycadopites* sporomorph assemblage (Qu et al., 1980; Qu et al., 1982; Tong et al., 2019). There are also some bivalves, some ophiurids and the *Leptolimnadia-Paleoleptestheria* conchostracan assemblage in the Qishan Formation (Figs. 9G and 9R; Supplemental Data File 5;

Downloaded from http://pubs.geoscienceworld.org/gsa/gsabulletin/article-pdf/doi/10.1130/B36316.1/5749686/b36316.pdf
by University of Bristol user

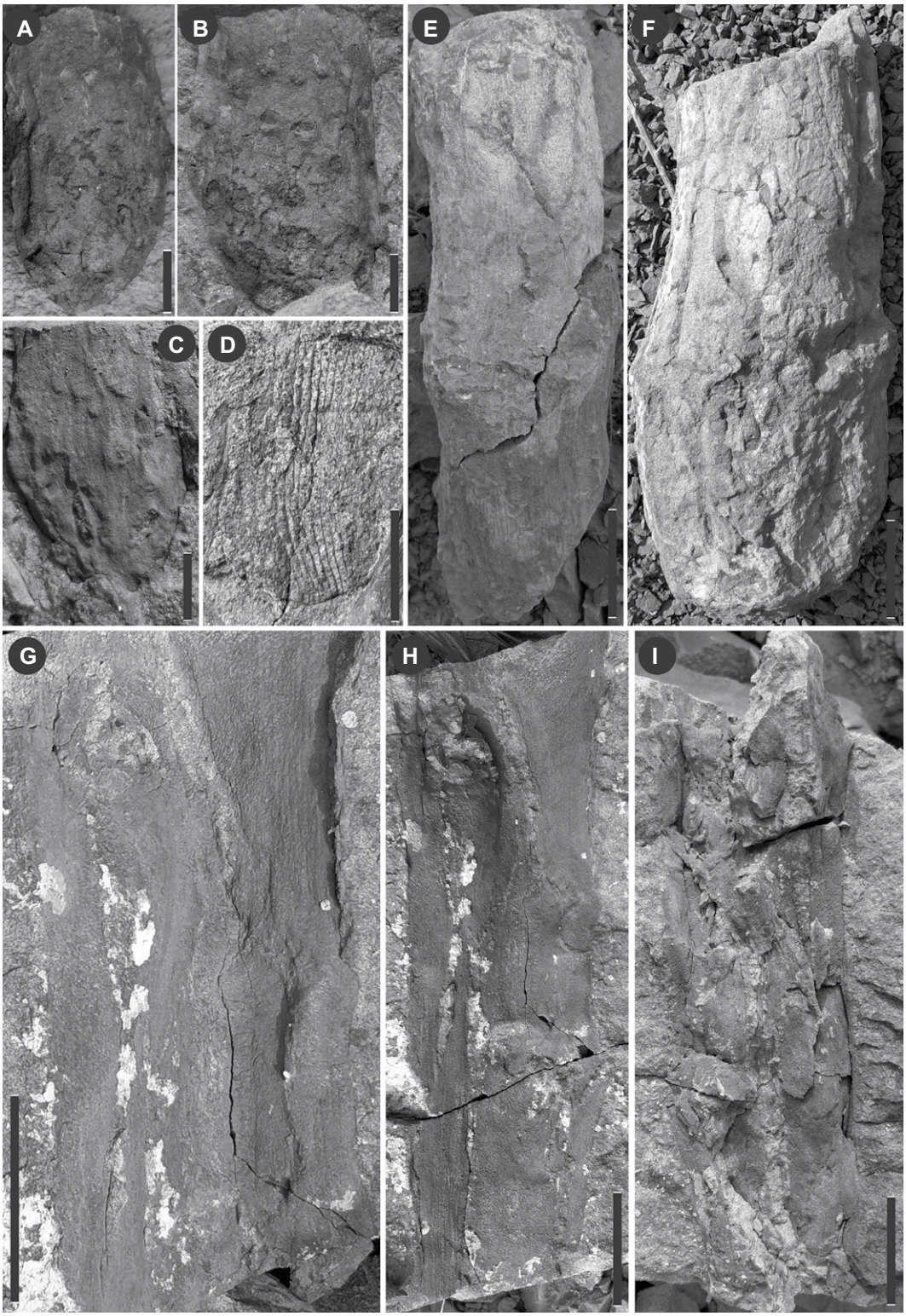

Figure 8. Some plant fossils from the Ermaying Formation of the Yushe section in North China. (A–C) Some rhizophores of *Pleuromeia*. (D–F) Some broken sphenophyte stems of probable *Neocalamites*, showing possible invertebrate burrows inside the cast of the stem in F. (G–I) Some woody plant fossil wood casts. Scale bars: A–D are 1 cm; E–I are 5 cm.

Tong et al., 2019), all of which indicate an early Olenekian age.

Subsequently, the lower part of the Heshanggou Formation is characterized by the *Pleuromeia-Tongchuanophyllum* flora that is associated with a few tetrapod fossils (e.g., Capitosauridae) (Wang, 1983) and the *Cornia-Estheriella* conchostracan assemblage (Wang, 1983). Higher up in the middle-upper parts of the Heshanggou Formation and basal Ermaying Formation, sporomorphs are assigned to the *Lundbladispora–Verrucosisporites–Lunatisporites* sporomorph assemblage and occur along with the macroflora documented above (Qu et al., 1980; Ouyang and Norris, 1988; Tong et al., 2019). The sporomorph assemblage includes a higher proportion of gymnosperm pollen (*Cycadopites* and *Lunatisporites*) (Ouyang and Norris, 1988).

Downloaded from http://pubs.geoscienceworld.org/gsa/gsabulletin/article-pdf/doi/10.1130/B36316.1/5749686/b36316.pdf
by University of Bristol user

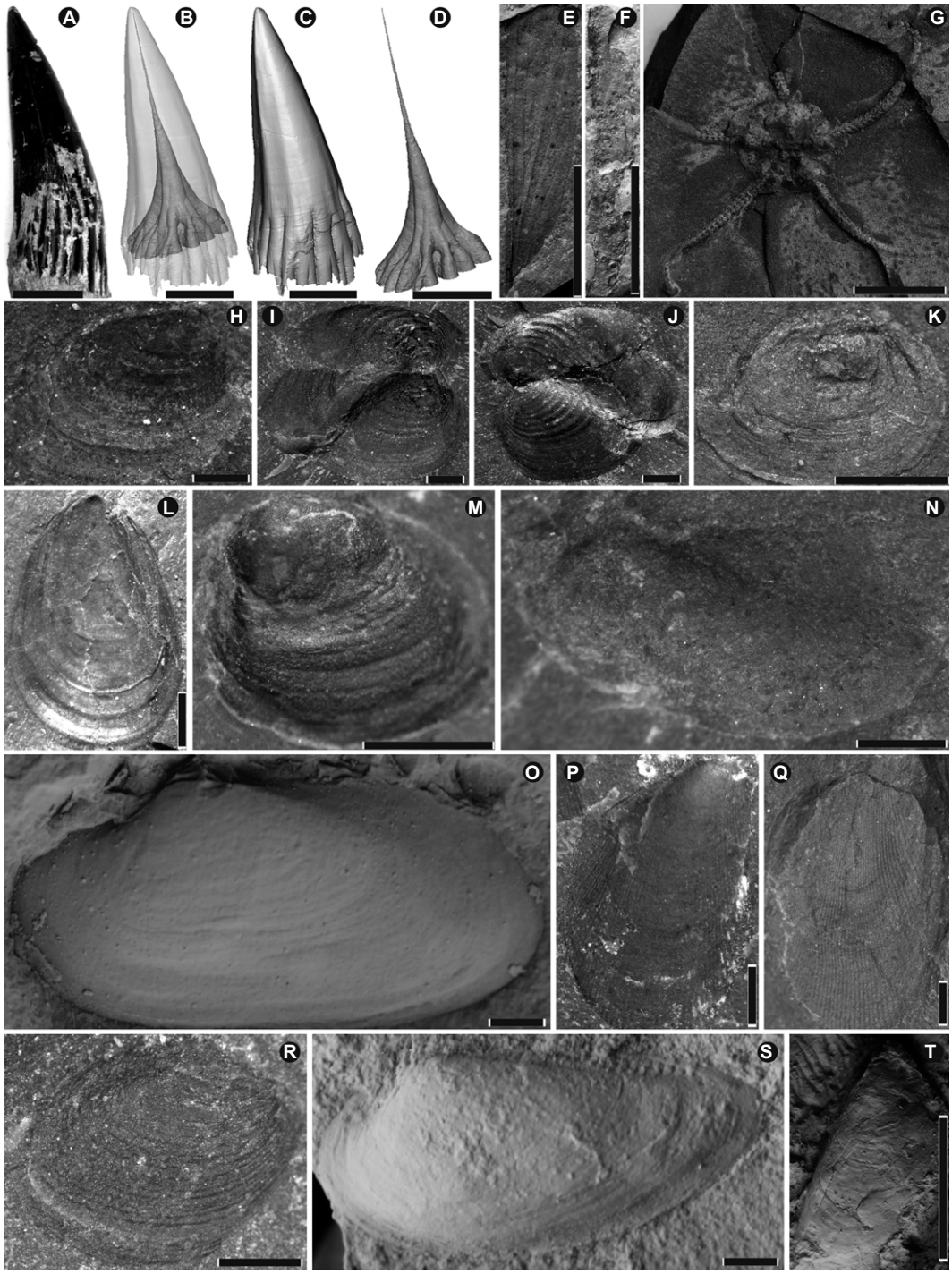

Figure 9. Other fossils associated with fossil plants. (A–D) CT scanned 3-D photos of a Temnospondyli tooth from the fossil-plant-bearing horizon of the Upper Shihhotse Formation in the Shichuanhe section in North China showing a well-preserved inner structure; (E) fragment of an insect wing fossil; (F) many microconchids found on some plant remains; (G) some ophiurids; (H–K, M, and R) some conchostracans (H–K, *Pseudestheria* spp.; M, *Euestheria gutta*; R, *Magniestheria mangaliensis*); (L) some lingulids; (N–Q, S, and T) some bivalves (N, *Pteria ussurica variabilis*; O, *Wilkingia* sp.; P, *Modiolus* sp.; Q, *Leptochondria* sp.; S, *Palaeoneilo elliptica*; T, *Promyalina putiatinensis*). Scale bars: A–G, O, P, and T are 1 cm; H–N and Q–S are 1 mm. E, F, and L–N were found in the rich sporomorph horizon of the Sunjiagou Formation in the Shichuanhe section; G and R were found in a rich sporomorph horizon of the Qishan Formation in the Zishiya section; H–K were found with fossil plants in the Lower Sunjiagou Formation, H–J, in the Liulin section; K, in the Dayulin section; O–Q, S, and T were found in the fossil-plant-bearing horizon of the Sunjiagou Formation in the Zishiya section.

In addition, vertebrate fossils (including the lungfish *Ceratodus heshanggouensis*) increase in abundance (Wang, 1983; Supplemental Data File 7). Among invertebrates, abundant conchostracans of the *Magniestheria-Eosolimnadia* assemblage occur, together with abundant ostracod fossils of the *Darwinula triassiana–Darwinula fengfengensis–Darwinula rotundata* assemblage (Supplemental Data File 5, Pang, 1989; Tong et al., 2019). Thus, the age of most of the Heshanggou Formation should be Olenekian, except the uppermost part that hosts the *Shaanbeikannemeyeria* assemblage, which is assigned an Anisian age (Liu, 2018; Fig. S2; Supplemental Data File 7).

Finally, in the Ermaying Formation, the *Lepacyclotes-Voltzia* flora is associated with the *Punctatisporites-Chordasporites* sporomorph assemblage (Tong et al., 2019; Fig. S2; Supplemental Data Files 2 and 3). It co-occurs with abundant vertebrate and invertebrate fossils, i.e., the *Sinokannemeyeria–Parakannemeyeria–Shansiodon* tetrapod assemblage (Liu and Sullivan 2017; Liu et al., 2018; Fig. S2; Supplemental Data File 7), the *Brachyestheria-Xiangxiella* conchostracan assemblage (Tong et al., 2019), and the *Lutkevichinella minuta–Shensinella gaoyadiensis–Darwinula subovaliformis* ostracod assemblage (Tong et al., 2019; Fig. S2; Supplemental Data File 5). This biota indicates an Anisian age.

Downloaded from http://pubs.geoscienceworld.org/gsa/gsabulletin/article-pdf/doi/10.1130/B36316.1/5749686/b36316.pdf
by University of Bristol user

Permian to Middle Triassic Floral Changes

The Permian–Triassic mass extinction was the most severe event of the Phanerozoic, affecting both marine and continental organisms (Cascales-Miñana et al., 2016; Dal Corso et al., 2022). However, it has been debated whether there even was a mass extinction of land plants (Fielding et al., 2019; Nowak et al., 2019). In North China, it is well known that Permian lands were occupied by the famous *Gigantopteris* (Cathaysian) flora, which gradually went extinct in the later Permian (Hilton and Cleal, 2007; Wang, 2010; Stevens et al., 2011; Wu et al., 2021). There have been few investigations of paleofloral changes at other intervals through the Permian to Early-Middle Triassic (Wang, 1993, 1996, 2010; Stevens et al., 2011; Yang and Wang, 2012). A statistical analysis has been especially lacking. Here, we identify six statistically distinct floras through this interval (Figs. 10–12), separated by five floral transitions (T1–T5 in Fig. 10). Of these distinct floras, two are similar to each other, and they are regarded

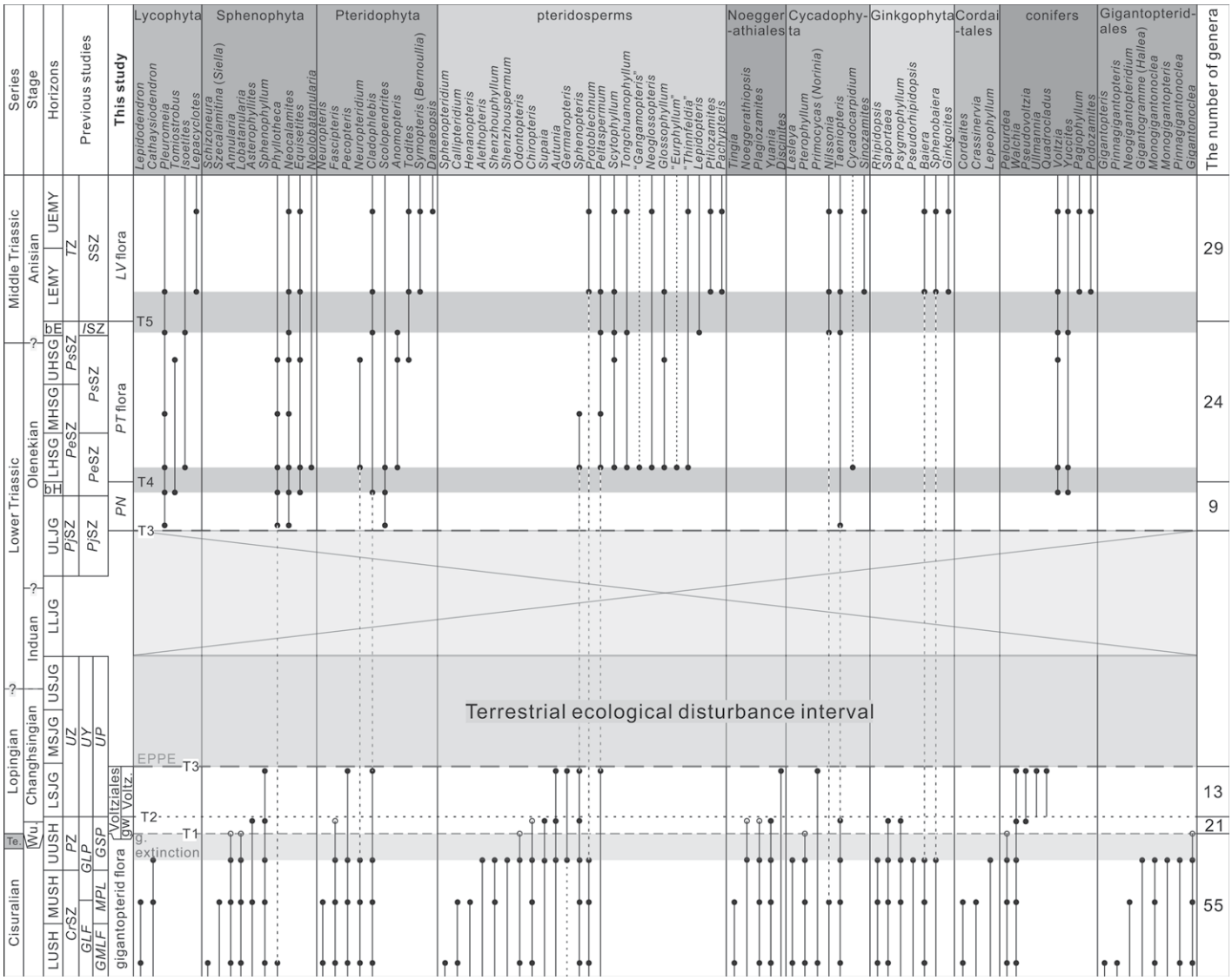

Figure 10. Range chart of floras from North China from the Cisuralian to Middle Triassic interval. Five floras, one of which includes two subfloras, and five floral transitions including an extirpation event, two turnovers, and two radiation events are recognized here (Supplemental Data Files 2 and 3; see footnote 1). g. extinction—gigantopterid flora extirpation; T1–T5—floral transition 1–5; EPPE—end-Permian plant extinction event. References of the previous studies can be seen in Supplemental Data File 4. Plant zones or subzones or assemblages in previous studies (see Supplemental Data File 4): *CrSZ*, *PZ*, *UZ*, *PjSZ*, *PeSZ*, *PsSZ*, *TZ*, *ISZ*, *SSZ*, *GLF*, *GLP*, *UY*, *GMLF*, *MPL*, *PSP*, *UP*; floras in this study (see Supplemental Data File 4): Voltziales—Voltziales flora; gw—ginkgophyte–walchian Voltziales subflora; Voltz.—voltzian Voltziales subflora; *PN—Pleuromeia–Neocalamites* flora; *PT* flora—*Pleuromeia–Tongchuanophyllum* flora; *LV* flora—*Lepacyclotes–Voltzia* flora. Te.—tectonism; Wu.—Wuchiapingian. UEMY—Upper Ermaying Formation; LEMY—Lower Ermaying Formation; bE—basal Ermaying Formation; UHSG—Upper Heshanggou Formation; MHSG—Middle Heshanggou Formation; LHSG—Lower Heshanggou Formation; bH—basal Heshanggou Formation; ULJG—Upper Liujiagou Formation; LLJG—Lower Liujiagou Formation; USJG—Upper Sunjiagou Formation; MSJG—Middle Sunjiagou Formation; LSJG—Lower Sunjiagou Formation; UUSH—Upper Upper Shihhotse Formation; MUSH—Middle Upper Shihhotse Formation; LUSH—Lower Upper Shihhotse Formation.

Downloaded from http://pubs.geoscienceworld.org/gsa/gsabulletin/article-pdf/doi/10.1130/B36316.1/5749686/b36316.pdf
by University of Bristol user

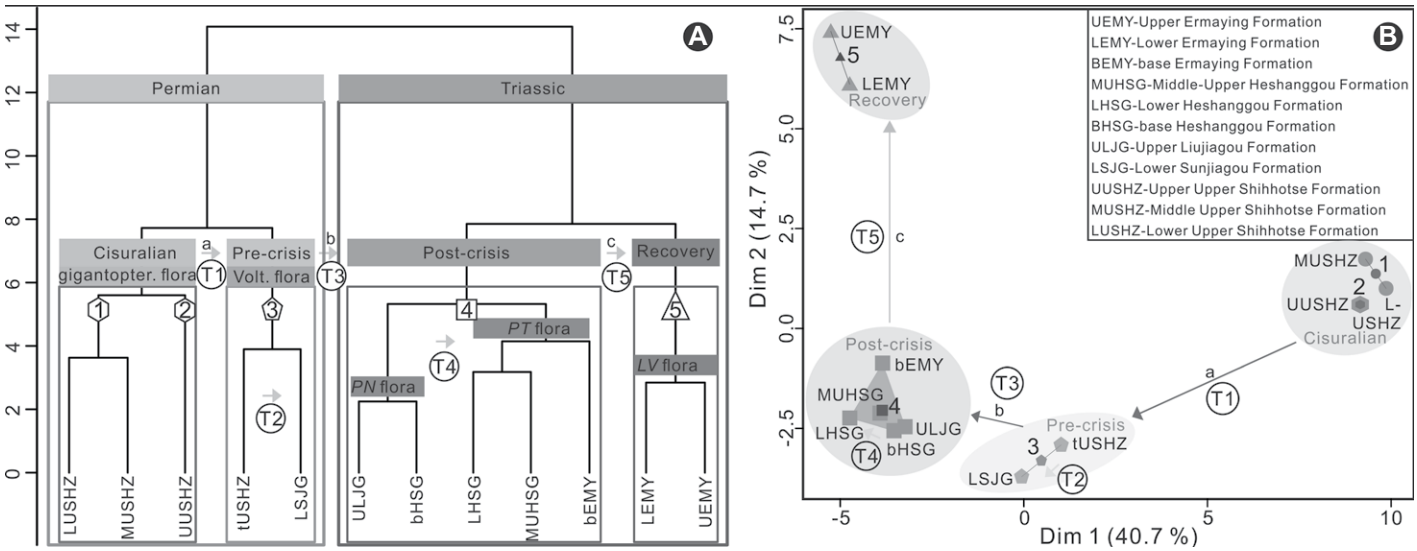

Figure 11. Hierarchical clustering and *k*-means clustering for five floras and three main phases from Permian to Middle Triassic in North China. (A) Hierarchical clustering-complete linkage analysis showing five different floras from Permian to Middle Triassic in North China; (B) k-means clustering analysis showing three main phases from Lopingian to Middle Triassic in North China. (A) The gigantopterid flora extirpation (T1) and the absence of the coal deposits, (B) end-Permian plant extinction (T3), and (C) gradual recovery of floras (T5). gigantopter. flora—gigantopterid flora; Volt. flora—Voltziales flora; *PN* flora—*Pleuromeia–Neocalamites* flora; *PT* flora—*Pleuromeia–Tongchuanophyllum* flora; *LV* flora—*Lepacyclotes–Voltzia* flora. 1–5—cluster centroids; T1–T5—floral transition 1–5.

as the sub-floras of one flora. These changes may help us to understand the Permian–Triassic transition of the plants on land in North China. In some instances, floral transitions are abrupt and can be well-defined by changes in composition at a particular level (represented by horizontal lines in Fig. 10). In other cases, the transitions span a broader time interval which may, in part, be due to low sampling frequency.

The first significant floral transition (T1) is recognized between the gigantopterid and Voltziales floras (Figs. 10 and 11B (a)). The gigantopterid flora was characterized by high diversity, including abundant and diverse gigantopterids, arborescent lycophytes, diverse sphenophytes, and "filicalean" ferns, abundant ginkgophytes, Noeggerathiales and Cordaitales but with few conifers. During this transition (Fig. 11B, from cluster 1 to cluster 2 and from cluster 2 to cluster 3) there is a decrease or the eventual loss of the dominant/characteristic elements, e.g., gigantopterids (Fig. 10). It is characterized by the disappearance of the Cathaysian flora (Wu et al., 2021) and a switch from the Cisuralian gigantopterid flora to the Lopingian Voltziales flora. This also marks the beginning of the Paleophytic to Mesophytic floral switch, which is a staggered event in our analysis. T1 marked the decline and eventual extirpation (regional extinction) of the gigantopterid flora (61.8% genera lost) and replacement by the incoming Voltziales flora that comprises taxa that ranged through this selective extinction event.

The second floral transition (T2) occurs within the Voltziales flora and is manifested as the turnover between the two subfloras (Figs. 10 and 11) in which 10 taxa disappear, two appear, and 11 range through the transition. The ginkgophyte–walchian Voltziales subflora (Figs. 10 and 11) is dominated by abundant walchian voltzialean conifers and early ginkgophytes, together with the cycad *Taeniopteris*, some pteridosperms (e.g., *Sphenopteris*, *Autunia*, *Supaia*), sphenophytes (e.g., *Sphenophyllum*), remaining ferns (e.g., *Pecopteris*), a few Noeggerathiales (e.g., *Yuania*), and a limited appearance of voltzian voltzialean conifers. Overall, the subflora is dominated by gymnosperms (>90%), rather than ferns, and it fits the broad characteristics of the "Mesophytic age" (Gothan, 1912; DiMichele et al., 2008). It is relatively different from the older gigantopterid-dominated flora in North China. So, it may be correlated with previously reported floras from the Upper Shihhotse Formation, such as the upper part of the *Psygmophyllum* zone (Wang, 1993), the post-changeover 4 flora (Wang, 2010) or the post-upper Upper Shihhotse Formation (uUSF) extinction flora (Stevens et al., 2011) (Fig. 10). However, there are some differences in the dominant elements in two subfloras of the Voltziales flora. The voltzian Voltziales subflora (Figs. 10 and 11) is dominated by voltzian voltzialean conifers, some pteridosperms, and a few sphenophytes and ferns. The presence of a diverse voltzian Voltziales assemblage with a few walchian Voltziales but no early ginkgophytes is especially noteworthy.

The third transition (T3) is more difficult to characterize and interpret as it comprises two stages separated by a broad interval lacking plant megafossils from the terrestrial ecological disturbance (TED) interval (see Xu et al., 2022). T3 commences with the disappearance of the latest Permian voltzian Voltziales subflora with 10/13 loss in genera across a wide range of plant groups (Figs. 10 and 11B (b)). This tran-

Figure 12. Model of floral community's changeovers associated with different animals during the Permian–Triassic crisis in North China. (1) *Tomiostrobus/Lepacyclotes*; (2) *Pleuromeia*; (3) Sphenophytes; (4 and 19) tree ferns; (5) small pteridophyte (e.g., *Anomopteris/Scolopendrites*); (6) pteridosperms; (7) cycads; (8) ginkgophytes; (9) conifers; (10) ostracods; (11) conchostracans; (12) Triopsidae; (13) bivalves; (14) insects; (15) fishes; (16) microbial-induced sedimentary structures; (17) lingulids; (18) *Yuania*; (20) gigantopterids; (21) Lepidodendrales. TED interval—terrestrial ecological disturbance interval; LMUUSHZ—Lower-Middle-Upper Shihhotse Formation; tUSHZ—topmost Upper Upper Shihhotse Formation; Fm.—Formation; g. extinction—gigantopterid flora extinction; T1–T5—floral transition 1–5; EPPE—end-Permian plant extinction event.

Downloaded from http://pubs.geoscienceworld.org/gsa/gsabulletin/article-pdf/doi/10.1130/B36316.1/5749686/b36316.pdf
by University of Bristol user

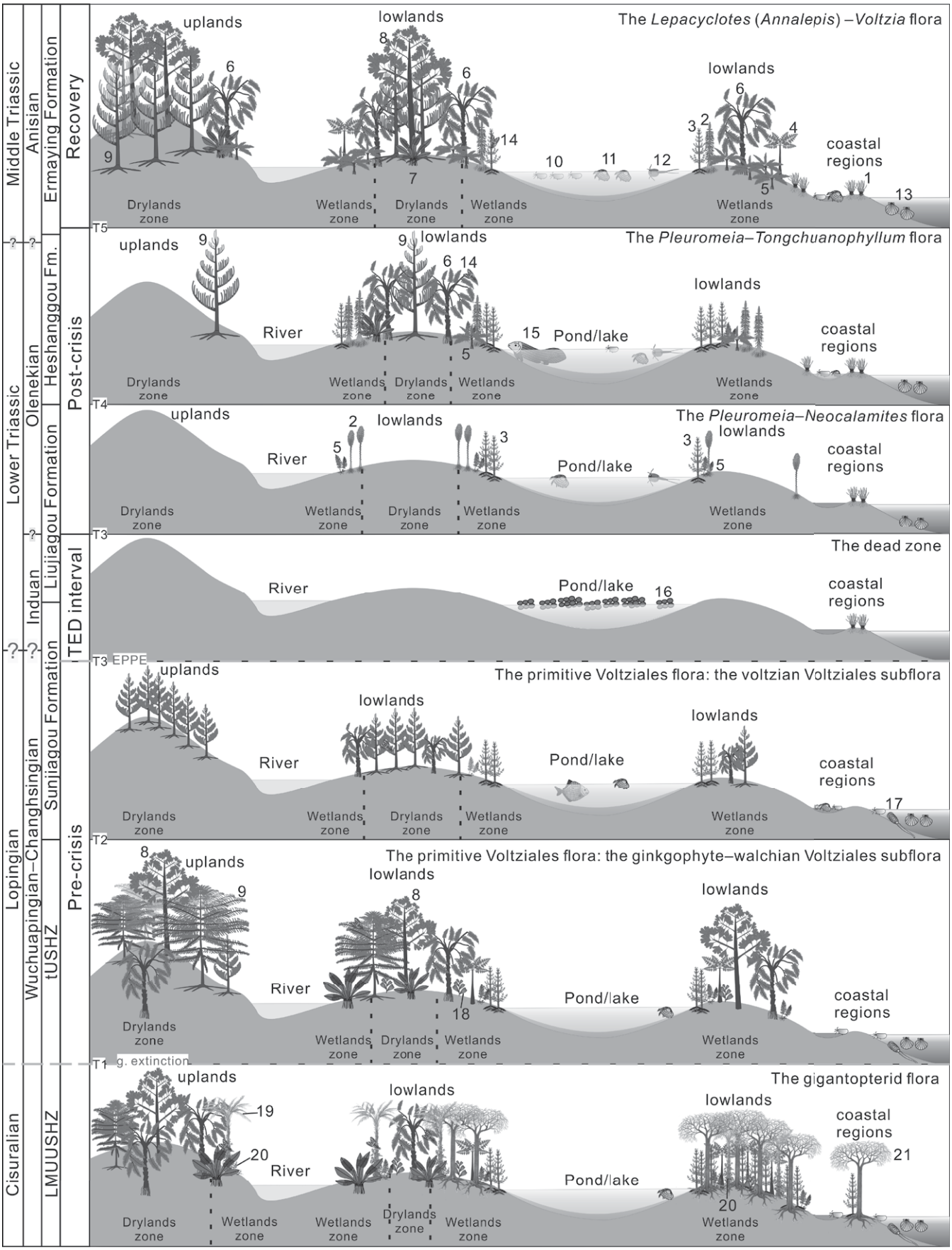

Downloaded from http://pubs.geoscienceworld.org/gsa/gsabulletin/article-pdf/doi/10.1130/B36316.1/5749686/b36316.pdf
by University of Bristol user

sition event (T3) can probably be regarded as the end Permian plant extinction (EPPE) (Xu et al., 2022) and the PTB plant mass extinction in North China, but it spans a wide time interval due to low sampling frequency (Fig. 10) and is best evidenced by the incoming Early Triassic flora. However, the duration of the crisis could be affected by poor preservation at this level in the TED interval. The dominantly red beds of mudstone and sandstone floodplain facies of the upper part of the Sunjiagou Formation provide a poor fossil plant record (see DiMichele et al., 2008). Such a scenario is supported by the absence of disaster floral elements such as *Pleuromeia*, which appears at a higher level, in the Liujiagou Formation, and the presence of pareiasaurs in the Sunjiagou Formation (Wang et al., 2019; Supplemental Data File 7) which suggests sufficient vegetation existed to support herbivorous vertebrates. Furthermore, the palynoflora from the basal Liujiagou Formation includes the voltzialean conifer pollen *Triadispora* (see Balme, 1995), suggesting that even though the voltzialean-dominated community disappeared in the megafossil record, the group was still present in the region. Plants from this community may not necessarily have been living in the floodplain depositional settings as conifer pollen is widely distributed (Ouyang and Zhang, 1982).

Following the initial loss of plant diversity in T3, the first megaflora of the Early Triassic, the *Pleuromeia–Neocalamites* flora (Fig. 12), is characterized by abundant *Pleuromeia* (typically *Pleuromeia jiaochengensis*) and common sphenophyte stems (*Neocalamites* and *Equisetites*) along with some pteridophytes and a few voltzian conifers (Fig. 10). We consider the appearance of this megaflora to mark the end of the third transition event (T3) (Fig. 10). An alternative interpretation might be to divide the T3 event as presented here into a separate Late Permian extinction event and an earliest Triassic radiation event. While future research is required to fully evaluate floral changes in transition, we consider this scenario less likely as the extinction and radiation appear intricately linked to the environmental perturbations of the TED interval.

The fourth floral transition (T4), from the *Pleuromeia–Neocalamites* to *Pleuromeia–Tongchuanophyllum* floras (Figs. 10 and 11A), represents a radiation event and short-term increase in gymnosperm diversity after the crisis in North China, characterized by the abrupt rise of pteridosperms and a few cycadophytes and conifers. The diversity of *Pleuromeia* also increased noticeably, whereas sphenophytes and pteridophytes increased only slightly (Fig. 10). This transition spans a wide time interval, probably due to low sampling frequency.

Finally, the final floral transition (T5) from the *Pleuromeia–Tongchuanophyllum* to the *Lepacyclotes–Voltzia* floras (Fig. 10 and 11B (c)) also spans a broad time interval due to low sampling frequency. In this radiation event many taxa co-occur in the *Pleuromeia–Tongchuanophyllum* and *Lepacyclotes–Voltzia* floras showing they are closely related to each other but are nonetheless distinct (Fig. 11). The latter flora is distinguished by a number of incoming pteridophytes, pteridosperms, cycadophytes, ginkgophytes, and conifers. The *Lepacyclotes–Voltzia* flora shows full recovery from the Permian–Triassic crisis in terms of diversity and abundance of nearly all higher taxa, including lycophytes, sphenophytes, pteridophytes, pteridosperms, cycadophytes, ginkgophytes, and conifers. Gymnosperms increased, especially ginkgophytes, cycadophytes, and conifers, and pteridophytes also diversified as tree ferns and ground ferns (Figs. 10–12).

During the Lopingian, floral distributions were latitude-dependent (Fig. 1A; Supplemental Data File 8), with four distinct floral provinces: the high-northern-latitude *Cordaites* peat-forming flora of the Angaran province (Davydov et al., 2021; Davydov and Karasev, 2021), the low-middle-northern-latitude voltzian Voltziales–pteridosperm floras (e.g., the voltzian Voltziales subflora in North China; Bourquin et al., 2011; Kustatscher et al., 2012, 2017; Cai et al., 2019), the tropical rainforest or lowland-peat-forming floras (e.g., the *Gigantopteris* flora in South China or the Umm Irna flora in Jordan; Yu et al., 2015; Blomenkemper et al., 2018; Feng et al., 2020), and the high-southern-latitude *Glossopteris* peat-forming flora in Gondwana (Fielding et al., 2019). During the Permian–Triassic mass extinction, floras changed dramatically globally. Early Triassic floras were sporadically distributed but with some widespread taxa (Fig. 1A). Herbaceous or shrub-like lycopsid-dominated floras, mainly *Tomiostrobus* and *Pleuromeia*, were widely distributed in the Northern Hemisphere (Fig. 1A; Supplemental Data File 8), and the *Lepidopteris*- and *Dicroidium*-dominated flora became established in the Southern Hemisphere (Fig. 1A; Supplemental Data File 8; Vajda et al., 2020).

Evolution of Terrestrial Ecosystems from Permian to Middle Triassic in North China

Here we discuss the evolution of the ecosystems on land through the Permian–Triassic transition, based on the fossil records of plants, sporomorphs, tetrapods, fishes, invertebrates, and trace fossils from North China. The transition was associated with turbulent environmental changes (Fig. 13), some of which led to biological responses, as highlighted by the hygrophyte/xerophyte ratio that reflects changes in floral composition from wet (hygrophyte) to dry (xerophyte) ecological settings (Supplemental Data Files 9 and 10).

The subsidence of the Cisuralian gigantopterid-dominated rainforest communities coincides with the last occurrence of coal deposits and the rise of the Lopingian ginkgophyte–walchian Voltziales forest community (Fig. 12) in North China. Disappearance of the *Gigantopteris* flora in North China represents a regional loss of diversity and an extirpation event because many taxa, but not all, and including the *Gigantopteris* flora, persisted in South China until the late Changhsingian where they were notable victims of the EPPC (e.g., Yu et al., 2015; Feng et al., 2020; Xu et al., 2022). In the meantime, the Jiyuan Fauna changed into the pareiasaur-dominated fauna while insect diversity decreased (Fig. 13; Supplemental Data Files 6 and 7; Xu et al., 2015; Wang et al., 2019). The gradual changeover in the *Gigantopteris* flora indicates increasing aridity, a trend that continues in the Voltziales flora (Fig. 13; Supplemental Data Files 9 and 10). A few insect remains (Fig. 9E) still co-occur with conifers in the top of the Upper Shihhotse and Sunjiagou formations (Fig. 2), and then there is no record of insect fossils from the point of disappearance of the Changhsingian conifer forests to the Middle Triassic in North China (Zheng et al., 2018). Both plant macrofossils and sporomorph records in the lower-middle parts of the Sunjiagou Formation were from voltzialean-dominated forests. The hygrophyte/xerophyte ratio indicates that arid or semi-arid conditions prevailed during the deposition of the lower-middle parts of the Sunjiagou Formation (Fig. 13). The mean annual precipitation was calculated, based on the depth to the Bk horizon in paleosols, as 320 ± 147 mm/yr (Yu et al., 2022).

The disappearance of the voltzian Voltziales-dominated forests (T3; Fig. 12) in the latest Changhsingian, is commonly associated with the appearance of red beds and MISS in lacustrine facies (Chu et al., 2015). However, despite the apparent forest floral crisis of the EPPC, some tetrapods persisted in the Upper Sunjiagou Formation (Fig. 2, Liulin section; Fig. 13) as did aquatic invertebrates, such as the conchostracans *Palaeolimnadia* and *Euestheria* and ostracods *Darwinula* and *Panxiania* (Fig. 13; Supplemental Data Files 5 and 7, Chu et al., 2015). The Voltziales-dominated flora may have persisted in the latest Changhsingian, at the same time as the tetrapod losses, but poor preservation could have "back-smeared" the final occurrence.

The Early Triassic (Induan?) *Aratrisporites–Alisporites* sporomorph assemblage (Ouyang

Downloaded from http://pubs.geoscienceworld.org/gsa/gsabulletin/article-pdf/doi/10.1130/B36316.1/5749686/b36316.pdf
by University of Bristol user

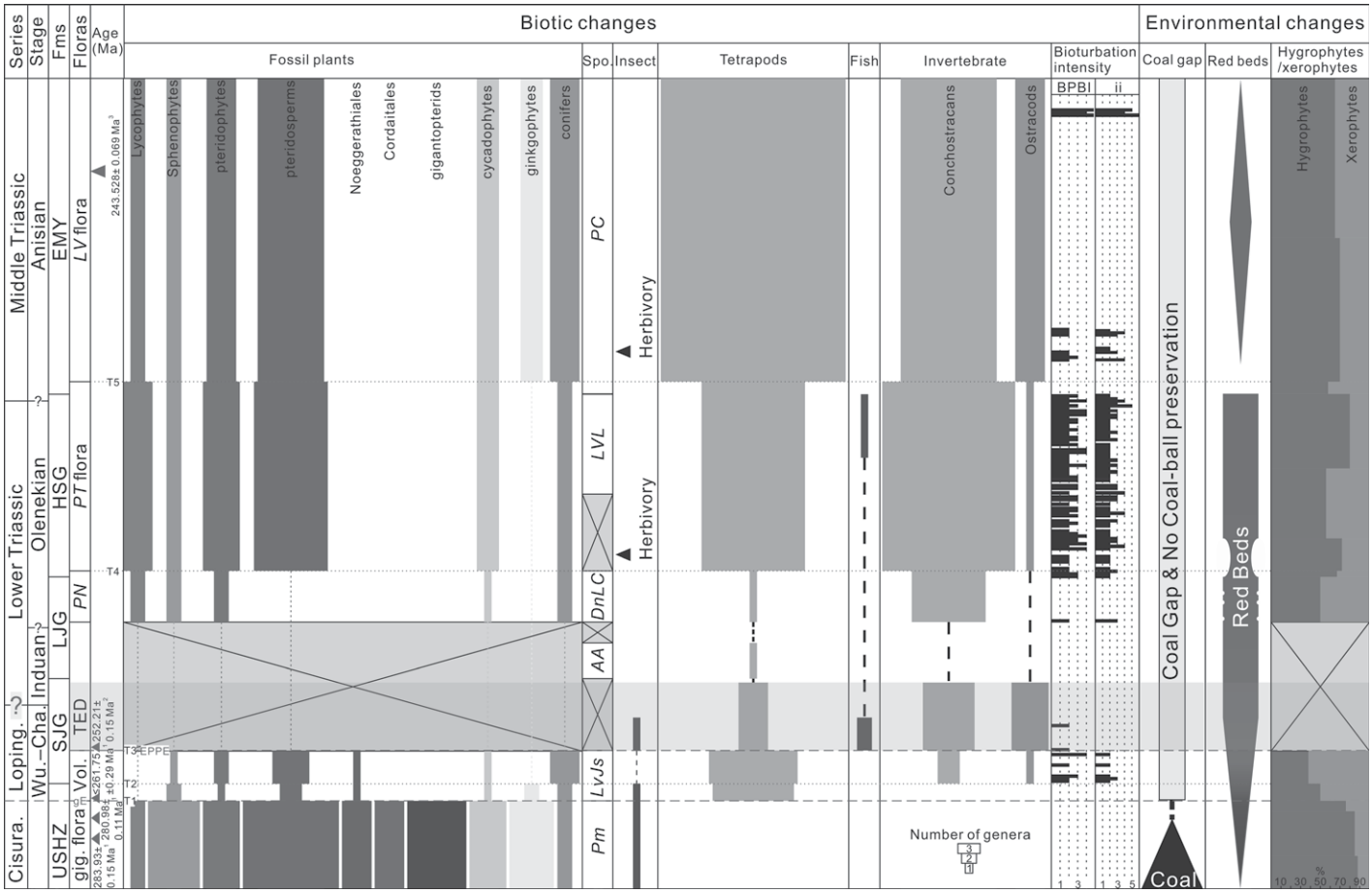

Figure 13. Late Permian to Triassic biotic and environmental changes in North China. Including diversity of plant, insect, tetrapod, fish, invertebrate, and trace fossils associated with the environmental changes of coal deposits, red beds, and humid/arid climates. Changes of coal deposits and red beds are modified from Wang (2010) and other data are in Supplemental Data Files 2–9 (see footnote 1). Fms—Formations; USHZ—Upper Shihhotse Formation; SJG—Sunjiagou Formation; LJG—Liujiagou Formation; HSG—Heshanggou Formation; EMY—Ermaying Formation; Spo.—sporomorph assemblages; Cisura.—Cisuralian; Loping.—Lopingian; Wu.–Cha.—Wuchiapingian–Changhsingian. TED interval is the terrestrial ecological disturbance interval; gig. flora—gigantopterid flora; Vol. flora—Voltziales flora; *PN* flora—*Pleuromeia–Neocalamites* flora; *PT* flora—*Pleuromeia–Tongchuanophyllum* flora; *LV* flora—*Lepacyclotes–Voltzia* flora. Sporomorph assemblages: *Pm—Patellisporites meishanensis* biozone; *LvJs—Lueckisporites virkkiae–Jugasporites schaubergeroides* assemblage; *AA—Aratrisporites–Alisporites* assemblage; *DnLC—Densoisporites nejburgii–Lunatisporites–Cycadopites* assemblage; *CLV—Cycadopites–Lunatisporites–Verrucosisporites* assemblage; *PC—Punctatisporites–Chordasporites* assemblage, see in Fig. S2 (see footnote 1). The bioturbation intensity bedding plane bioturbation index (BPBI) and ichnofabric index (ii) data are from Guo et al. (2019). Dashed lines mark the position of two losses of diversity, the lowermost an extirpation event and the upper extinctions of the end-Permian plant extinction event (EPPC); three dotted lines mark the positions of three transitions: the lowermost a turnover and the upper two radiations; gE—gigantopterid flora extirpation; T1–T5—floral transition 1–5.

and Zhang, 1982) may represent the first herbaceous lycopsid plant community occupying lowlands, coexisting with a few upland gymnosperms (Fig. 12), established after the crisis. This was followed by the early Olenekian *Pleuromeia–Neocalamites* flora representing *Pleuromeia*/*Neocalamites*-dominated shrub marshes in muddy wetlands. These occur in situ in sandstones or silty mudstones of the Liujiagou Formation and the base of the Heshanggou Formation (Figs. S1H and S1I), interpreted as braided river and shallow lake environments (Ji et al., 2021). *Pleuromeia*/*Neocalamites*-dominated shrub marshes likely grew in riverbank or muddy floodplain settings. In the late stage of the *Pleuromeia–Neocalamites* flora, a few *Voltzia* conifer shrubs appeared and might have grown in well-drained sandy riverbanks. Some allochthonous fragments of *Tomiostrobus* may have been derived from sporadically distributed plants around small ephemeral water bodies. Concurrently, aquatic invertebrates appeared in this ecosystem, such as conchostracans, ostracods, and Triopsidae (Wang, 1983). The hygrophyte/xerophyte ratio indicates a more humid environment in the early Olenekian than during the latest Changhsingian in North China (Fig. 13; Supplemental Data Files 9 and 10), which is consistent with geochemical data from paleosols in North China (Yu et al., 2022).

Subsequently, in the *Pleuromeia–Tongchuanophyllum* flora, pteridosperm-conifer shrub woodlands are identified by the appearance of abundant pteridosperms ("*Euryphyllum,*" "*Gangamopteris,*" *Glossophyllum*, *Neoglossopteris*, *Sphenopteris*, "*Thinnfeldia,*"

Downloaded from http://pubs.geoscienceworld.org/gsa/gsabulletin/article-pdf/doi/10.1130/B36316.1/5749686/b36316.pdf
by University of Bristol user

Tongchuanophyllum, *Peltaspermum*, and *Scytophyllum*) and some *Voltzia* elements (Fig. 12). Lacustrine conditions were predominant in this stage (Hu et al., 2009). These *Voltzia*-dominated woodland communities grew in well-drained sandy-soil riverbanks or other lowlands (Fig. 12). The lycophyte (*Pleuromeia*)–sphenophyte (*Neocalamites*, *Equisetites* and *Phyllotheca*)-dominated shrub marsh community with some pteridophytes (e.g., *Todites*, *Neuropteridium*, and *Anomopteris*) was still widely distributed on riverbanks or muddy floodplains (Fig. 12). Some *Tomiostrobus*-dominated, herbaceous, ground-covering communities occurred around the shores of playa lakes. In addition, some insect herbivory damage appeared on leaves of *Tongchuanophyllum* (Fig. 7O), and abundant small, spiral microconchid-like organisms on sporophylls of *Pleuromeia* (Fig. 7D) are preserved. Moreover, many vertebrate fossils (Benthosuchidae, Capitosauridae, Procolophonidae, Scaloposauria, *Eumetabolodon*, *Fugusuchus*, *Hazhenia*, *Pentaedrusaurus*, and *Xilousuchus*), some fish (*Ceratodus*) and many invertebrates co-occur with this flora (Wang, 1983; Nesbitt et al., 2011; Fig. 13; Supplemental Data File 7). All these changes suggest that diverse terrestrial and aquatic ecosystems had begun to reappear (Fig. 12). At this time, there are abundant types of trace fossils in continental ecosystems (Fig. 13, Shu et al., 2018; Guo et al., 2019) recording widespread activity on land, as well as posture changes and the evolution of endothermy with insulation (hair, feathers) in synapsid and archosauromorph tetrapods (Benton, 2021). The increase of invertebrate diversity (Fig. 13) may indicate a repopulation of aquatic ecosystems following their disappearance in the late Changxingian. Sporomorphs in the later stages of this flora are represented by the *Cycadopites–Lunatisporites–Verrucosisporites* sporomorph assemblage, and the hygrophyte/xerophyte ratio indicates a relatively seasonally humid environment in the late Olenekian (Fig. 13; Supplemental Data Files 9 and 10) and the mean annual precipitation was calculated to range from 520 ± 147 mm/yr to 680 ± 147 mm/yr (Yu et al., 2022).

In the *Lepacyclotes–Voltzia* flora, some xerophytic gymnosperms (e.g., *Lepidopteris*, *Peltaspermum*, *Pagiophyllum*, *Yuccites*, and *Voltzia*) started to occupy some dry uplands (Fig. 12) if they were not already established there; such absences may represent a taphonomic bias toward wetland depositional settings (see Blomenkemper et al., 2018). Along with the increased diversity of pteridophytes, pteridosperms, cycadophytes, ginkgophytes, and conifers, the gymnosperm-dominated forest community started to occupy some dry uplands, and the pteridophyte-dominated shrub community entered moist lowlands. The *Pleuromeia*–sphenophyte-dominated shrub marsh community was still on riverbanks or muddy floodplains (Fig. 12). At that time, the *Sinokannemeyeria* fauna was widely distributed in North China (Liu and Sullivan, 2017). Aquatic invertebrates probably also increased (Figs. 12 and 13), as also suggested by abundant burrows inside the cast of *Neocalamites* (Fig. 8F). The hygrophyte/xerophyte ratio indicates a gradual shift to a more humid climate (Fig. 13; Supplemental Data Files 9 and 10).

CONCLUSION

A new integrated multifaceted biostratigraphic framework with a refined time scale is established for the Lopingian–Middle Triassic of North China, based on macrofossil plant, sporomorph, vertebrate, and invertebrate (conchostracans and ostracodes) assemblages.

Five main floras are recognized and identified in North China, the gigantopterid, Voltziales, *Pleuromeia–Neocalamites*, *Pleuromeia–Tongchuanophyllum*, and *Lepacyclotes–Voltzia* floras, with the Voltziales flora comprising the ginkgophyte–walchian Voltziales and the voltzian Voltziales subfloras. The five transitions between these floras consist of an extirpation event, two turnover events, and two radiation events. The gigantopterid flora regional extinction (T1; 34/55 genera lost) eliminated the gigantopterid-dominated rainforest and saw the end of coal deposition. This marks the beginning of the changeover from the Paleophytic to Mesophytic floras. The second floral transition (T2), is a subflora turnover within the Voltziales flora, and saw a change in the dominant elements. The end-Permian plant extinction event (EPPE; T3), which saw the loss of 10 out of 13 genera, marks the start of the terrestrial ecological disturbance interval (TED interval) on land. This crisis was followed by a short-term diversification (T4) from the *Pleuromeia–Neocalamites* to the *Pleuromeia–Tongchuanophyllum* floras. The final floral transition (T5) in the earliest Middle Triassic, indicating the recovery-radiation of plants, represented by the *Lepacyclotes–Voltzia* flora, shows the initial construction of the Mesophytic Flora.

From the Cisuralian to Lopingian, the change from a gigantopterid-dominated rainforest community to a voltzialean conifer forest community occurred in parallel with the decline of the Jiyuan fauna and change to a pareiasaur-dominated fauna, loss of coal deposits, sharp increase of red beds, and aridity increase. The subsequent disappearance of the voltzialean conifer forest community marks the end-Permian plant extinction in North China. Following the prolonged plant-free terrestrial ecological disturbance interval the first plants to recover after the crisis belonged to a herbaceous plant community, followed by a *Pleuromeia–Neocalamites* shrub marsh community. A pteridosperm shrub woodland community dominated for a short time in the late Early Triassic, along with the first appearance of insect herbivory. Finally, in the Middle Triassic, the gymnosperm forest community gradually rose to dominance with the appearance of diverse plant communities on lowland and possible upland settings.

ACKNOWLEDGMENTS

This study was jointly funded by the National Natural Science Foundation of China (grant numbers 9205520023, 42030513, 41661134047, and 41530104) and the UK Natural Environment Research Council's Eco-PT project (NE/P01377224/1) to P.B.W., M.J.B., and J.H. We thank our colleagues, Yuyang Wu, Yingyue Yu, Wenwei Guo, Kaixuan Ji, Xue Miao, Meijia Zhang, Zhen Xu, Xin Sun, Qing Xue, Yuyang Tian, and Yan Ye for help in the field and general advice. Especially, we thank Patrick Blomenkemper and Hans Kerp for guidance on cuticular analysis, Jacopo Dal Corso for many constructive suggestions and Weidong Liu of Shanxi Institute of Geological Survey for help with the reference "*Triassic of Shanxi.*" We thank the editors Wenjiao Xiao and Ganqing Jiang for their editions and reviews. In addition, we also thank four anonymous reviewers for feedback on the manuscript.

REFERENCES CITED

Balme, B., 1995, Fossil in-situ spores and pollen grains: An annotated catalogue: Review of Palaeobotany and Palynology, v. 87, p. 81–323, https://doi.org/10.1016/0034-6667(95)93235-X.

Benton, M.J., 2016, The Chinese pareiasaurs: Zoological Journal of the Linnean Society, v. 177, p. 813–853, https://doi.org/10.1111/zoj.12389.

Benton, M.J., 2018, Hyperthermal-driven mass extinctions: killing models during the Permian–Triassic mass extinction: Philosophical Transactions of the Royal Society A, v. 376, https://doi.org/10.1098/rsta.2017.0076.

Benton, M.J., 2021, The origin of endothermy in synapsids and archosaurs and arms races in the Triassic: Gondwana Research, v. 100, p. 261–289, https://doi.org/10.1016/j.gr.2020.08.003.

Benton, M.J., and Newell, A.J., 2014, Impacts of global warming on Permo-Triassic terrestrial ecosystems: Gondwana Research, v. 25, p. 1308–1337, https://doi.org/10.1016/j.gr.2012.12.010.

Blomenkemper, P., Kerp, H., Hamad, A.A., DiMichele, W.A., and Bomfleur, B., 2018, A hidden cradle of plant evolution in Permian tropical lowlands: Science, v. 362, p. 1414–1416, https://doi.org/10.1126/science.aau4061.

Bourquin, S., Bercovici, A., López–Gómez, J., Diez, J.B., Broutin, J., Ronchi, A., Durand, M., Arche, A., Linol, B., and Amour, F., 2011, The Permian–Triassic transition and the onset of Mesozoic sedimentation at the northwestern peri-Tethyan domain scale: Palaeogeographic maps and geodynamic implications: Palaeogeography, Palaeoclimatology, Palaeoecology, v. 299, p. 265–280, https://doi.org/10.1016/j.palaeo.2010.11.007.

Broutin, J., Roger, J., Platel, J.-P., Angiolini, L., Baud, A., Bucher, H., Marcoux, J., and Al Hasmi, H., 1995, The Permian Pangea: Phytogeographic implications of new paleontological discoveries in Oman (Arabian Peninsula): Comptes Rendus de l'Academie des Sciences Paris: Série Iia, v. 321, p. 1069–1086.

Downloaded from http://pubs.geoscienceworld.org/gsa/gsabulletin/article-pdf/doi/10.1130/B36316.1/5749686/b36316.pdf
by University of Bristol user

Broutin, J., Yu, J.X., Shi, X., Shu, W.C., and Qing, X., 2020, Terrestrial palaeofloral succession across the Permian–Triassic Boundary in the North and South China blocks: a brief review: Palaontologische Zeitschrift, v. 94, p. 633–644, https://doi.org/10.1007/s12542-020-00511-0.

Cai, Y.F., Zhang, H., Feng, Z., Cao, C.Q., and Zheng, Q.F., 2019, A *Germaropteris*-dominated flora from the upper Permian of the Dalongkou section, Xinjiang, Northwest China, and its paleoclimatic and paleoenvironmental implications: Review of Palaeobotany and Palynology, v. 266, p. 61–71, https://doi.org/10.1016/j.revpalbo.2019.01.006.

Cascales-Miñana, B., Diez, J.B., Gerrienne, P., and Cleal, C.J., 2016, A palaeobotanical perspective on the great end-Permian biotic crisis: Historical Biology, v. 28, p. 1066–1074, https://doi.org/10.1080/08912963.2015.1103237.

Chaloner, W.G., and Lacey, W.A., 1973, The distribution of Late Palaeozoic floras, *in* Hughes, N.F., ed., Organisms and Continent Through Time: Special Papers in Palaeontology, Palaeontological Association, London, v. 12, p. 271–290.

Chu, D.L., Tong, J.N., Song, H.J., Benton, M.J., Bottjer, D.J., Song, H.Y., and Tian, L., 2015, Early Triassic wrinkle structures on land: Stressed environments and oases for life: Scientific Reports, v. 5, https://doi.org/10.1038/srep10109.

Chu, D.L., Tong, J.N., Benton, M.J., Yu, J.X., and Huang, Y.F., 2019, Mixed continental-marine biotas following the Permian–Triassic mass extinction in South and North China: Palaeogeography, Palaeoclimatology, Palaeoecology, v. 519, p. 95–107, https://doi.org/10.1016/j.palaeo.2017.10.028.

Chu, D.L., Grasby, S.E., Song, H.J., Corso, J.D., Wang, Y., Mather, T.A., Wu, Y.Y., Song, H.Y., Shu, W.C., Tong, J.N., and Wignall, P.B., 2020, Ecological disturbance in tropical peatlands prior to marine Permian–Triassic mass extinction: Geology, v. 48, p. 288–292, https://doi.org/10.1130/G46631.1.

Cleal, C.J., and Cascales-Miñana, B., 2014, Composition and dynamics of the great Phanerozoic Evolutionary Floras: Lethaia, v. 47, p. 469–484, https://doi.org/10.1111/let.12070.

Cleal, C.J., Pardoe, H.S., Berry, C.M., Cascales-Miñana, B., Davis, B.A.S., Diez, J.B., Filipova-Marinova, M.V., Giesecke, T., Hilton, J., Ivanov, D.A., Kustatscher, E., Leroy, S.A.G., McElwain, J.C., Opluštil, S., Popa, M.E., Seyfullah, L.J., Stolle, E., Thomas, B.A., and Uhl, D., 2021, Plant diversity in deep time: 1. How well can we identify past plant diversity in the fossil record?: Palaeogeography, Palaeoecology, Palaeoclimatology, v. 576, https://doi.org/10.1016/j.palaeo.2021.110481.

Dal Corso, J., Song, H.J., Callegaro, S., Chu, D.L., Sun, Y.D., Hilton, J., Grasby, S.E., Joachimski, M.M., and Wignall, P.B., 2022, Environmental crises at the Permian–Triassic mass extinction: Nature Reviews. Earth & Environment, v. 3, p. 197–214, https://doi.org/10.1038/s43017-021-00259-4.

Davydov, V.I., and Karasev, E.V., 2021, The influence of the Permian-Triassic magmatism in the Tunguska Basin, Siberia on the regional floristic biota of the Permian-Triassic transition in the region: Frontiers of Earth Science, v. 9, https://doi.org/10.3389/feart.2021.635179.

Davydov, V.I., Karasev, E.V., Nurgalieva, N.G., Schmitz, M.D., Budnikov, I.V., Biakov, A.S., Kuzina, D.M., Silantiev, V.V., Urazaeva, M.N., Zharinova, V.V., and Zorina, S.O., 2021, Climate and biotic evolution during the Permian-Triassic transition in the temperate Northern Hemisphere, Kuznetsk Basin, Siberia, Russia: Palaeogeography, Palaeoclimatology, Palaeoecology, v. 573, https://doi.org/10.1016/j.palaeo.2021.110432.

DiMichele, W.A., Kerp, H., Tabor, N.J., and Looy, C.V., 2008, The so-called "Paleophytic–Mesophytic" transition in equatorial Pangea: Multiple biomes and vegetational tracking of climate change through geological time: Palaeogeography, Palaeoclimatology, Palaeoecology, v. 268, p. 152–163, https://doi.org/10.1016/j.palaeo.2008.06.006.

DiMichele, W.A., Bashforth, A.R., Falcon-Lang, H.J., and Lucas, S.G., 2020, Uplands, lowlands, and climate: Taphonomic megabiases and the apparent rise of a xeromorphic, drought-tolerant flora during the Pennsylvanian-Permian transition: Palaeogeography, Palaeoclimatology, Palaeoecology, v. 559, https://doi.org/10.1016/j.palaeo.2020.109965.

Feng, Z., Wei, H.-B., Guo, Y., He, X.Y., Sui, Q., Zhou, Y., Liu, H.Y., Gou, X.D., and Lü, Y., 2020, From rainforest to herbland: New insights into land plant responses to the end–Permian mass extinction: Earth-Science Reviews, v. 204, https://doi.org/10.1016/j.earscirev.2020.103153.

Fielding, C.R., Frank, T.D., McLoughlin, S., Vajda, V., Mays, C., Tevyaw, A.P., Winguth, A., Winguth, C., Nicoll, R.S., Bocking, M., and Crowley, J.L., 2019, Age and pattern of the southern high-latitude continental end-Permian extinction constrained by multiproxy analysis: Nature Communications, v. 10, no. 385, https://doi.org/10.1038/s41467-018-07934-z.

Foster, C.B., and Afonin, S.A., 2005, Abnormal pollen grains: an outcome of deteriorating atmospheric conditions around the Permian–Triassic boundary: Journal of the Geological Society, v. 162, p. 653–659, https://doi.org/10.1144/0016-764904-047.

Frank, T.D., Fielding, C.R., Winguth, A.M.E., Savatic, K., Tevyaw, A., Winguth, C., McLoughlin, S., Vajda, V., Mays, C., Nicoll, R., and Bocking, M., 2021, Pace, magnitude, and nature of terrestrial climate change through the end-Permian extinction in southeastern Gondwana: Geology, v. 49, p. 1089–1095, https://doi.org/10.1130/G48795.1.

Gastaldo, R.A., Kamo, S.L., Neveling, J., Geissman, J.W., Looy, C.V., and Martini, A.M., 2020, The base of the *Lystrosaurus* Assemblage Zone, Karoo Basin, predates the end-Permian marine extinction: Nature Communications, v. 11, no. 1428, https://doi.org/10.1038/s41467-020-15243-7.

Gothan, W., 1912, Paläobotanik, *in* Korschelt, E., Linck, G., Schaum, K., Simon, H. Th., Verworn, M., and Teichmann, E., eds., Handwörterbuch der Naturwissenschaften [in German]: Jena, Germany, Gustav Fischer Verlag, p. 408–460.

Guo, W., 2022, Late Permian–Middle Triassic magnetostratigraphic timescale from terrestrial North China and secular variations of ichnofossils [Ph.D. thesis]: Wuhan, China, China University of Geosciences, 228 p.

Guo, W.W., Tong, J.N., Tian, L., Chu, D.L., Bottjer, D.J., Shu, W.C., and Ji, K.X., 2019, Secular variations of ichnofossils from the terrestrial Late Permian–Middle Triassic succession in the Shichuanhe section in Shaanxi Province, North China: Global and Planetary Change, v. 181, https://doi.org/10.1016/j.gloplacha.2019.102978.

Guo, W., Tong, J., He, Q., Hounslow, M.W., Song, H., Dal Corso, J., Wignall, P.B., Ramezani, J., Tian, L., and Chu, D., 2022, Late Permian–Middle Triassic magnetostratigraphy in North China and its implications for terrestrial-marine correlations: Earth and Planetary Science Letters, v. 585, https://doi.org/10.1016/j.epsl.2022.117519.

Hilton, J., and Cleal, C.J., 2007, The relationship between Euramerican and Cathaysian tropical floras in the Late Palaeozoic: Palaeobiogeographical and palaeogeographical implications: Earth-Science Reviews, v. 85, p. 85–116, https://doi.org/10.1016/j.earscirev.2007.07.003.

Hochuli, P.A., Sanson-Barrera, A., Schneebeli-Hermann, E., and Bucher, H., 2016, Severest crisis overlooked: Worst disruption of terrestrial environments postdates the Permian–Triassic mass extinction: Scientific Reports, v. 6, https://doi.org/10.1038/srep28372.

Hochuli, P.A., Schneebeli-Hermann, E., Mangerud, G., and Bucher, H., 2017, Evidence for atmospheric pollution across the Permian–Triassic transition: Geology, v. 45, p. 1123–1126, https://doi.org/10.1130/G39496.1.

Hou, J.P., and Ouyang, S., 2000, Palynoflora from the Sunjiagou Formation in Liulin County, Shanxi Province: Acta Palaeontologica Sinica, v. 39, p. 356–368.

Hu, B., Yang, W.T., Song, H.B., Wang, M., and Zhong, M.Y., 2009, Trace fossils and ichnofabrics in the Heshanggou Formation of lacustrine deposits, Jiyuan Area, Henan Province [in Chinese]: Chenji Xuebao, v. 27, p. 573–582.

Ji, K.X., Wignall, P.B., Peakall, J., Tong, J.N., Chu, D.L., and Pruss, S.B., 2021, Unusual intraclast conglomerates in a stormy, hot-house lake: The Early Triassic North China Basin: Sedimentology, v. 68, p. 3385–3404, https://doi.org/10.1111/sed.12903.

Ji, K.X., Wignall, P.B., Tong, J.N., Yu, Y.Y., Guo, W.W., Shu, W.C., and Chu, D.L., 2022, Sedimentology of the latest Permian to Early Triassic in the terrestrial settings of the North China Basin: Low-latitude climate change during a warming-driven crisis: Geological Society of America Bulletin, https://doi.org/10.1130/B36260.1.

Jones, T.P., and Rowe, N.P., 1999, Fossil Plants and Spores: Modern Techniques: Bath, UK, Geological Society of London, 420 p.

Kerp, H., 1990, The study of fossil gymnosperms by means of cuticular analysis: Palaios, v. 5, p. 548–569, https://doi.org/10.2307/3514861.

Koll, R.A., and DiMichele, W.A., 2021, Dominance-diversity architecture of a mixed hygromorphic-to-xeromorphic flora from a botanically rich locality in western equatorial Pangea (lower Permian Emily Irish site, Texas, USA: Palaeogeography, Palaeoclimatology, Palaeoecology, v. 563, https://doi.org/10.1016/j.palaeo.2020.110132.

Kustatscher, E., Van Konijnenburg-Van Cittert, J.H.A., Bauer, K., Butzmann, R., Meller, B., and Fischer, T.C., 2012, A new flora from the Upper Permian of Bletterbach (Dolomites, N-Italy): Review of Palaeobotany and Palynology, v. 182, p. 1–13, https://doi.org/10.1016/j.revpalbo.2012.06.001.

Kustatscher, E., Bernardi, M., Petti, F.M., Franz, M., Van Konijnenburg-Van Cittert, J.H.A., and Kerp, H., 2017, Sea-level changes in the Lopingian (late Permian) of the northwestern Tethys and their effects on the terrestrial palaeoenvironments, biota and fossil preservation: Global and Planetary Change, v. 148, p. 166–180, https://doi.org/10.1016/j.gloplacha.2016.12.006.

Lee, M.S.Y., 1997, A taxonomic revision of pareiasaurian reptiles: Implications for Permian terrestrial palaeoecology: Modern Geology, v. 21, p. 231–298.

Liu, J., 2018, New progress on the correlation of Chinese terrestrial Permo-Triassic strata: Vertebrata Palasiatica, v. 56, p. 327–342.

Liu, J., and Bever, G.S., 2018, The tetrapod fauna of the Upper Permian Naobaogou Formation of China: A new species of *Elginia* (Parareptilia, Pareiasauria): Papers in Palaeontology, v. 4, p. 197–209, https://doi.org/10.1002/spp2.1105.

Liu, J., and Sullivan, C., 2017, New discoveries from the *Sinokannemeyeria-Shansisuchus* Assemblage Zone: 3. Archosauriformes from Linxian, Shanxi, China: Vertebrata PalAsiatica, v. 55, p. 110–128.

Liu, J., Xu, L., Jia, S.H., Pu, H.Y., and Liu, X.L., 2014, The Jiyuan tetrapod fauna of the Upper Permian of China—2. stratigraphy, taxonomical review, and correlation: Vertebrata Palasiatica, v. 52, p. 328–339.

Liu, J., Ramezani, J., Li, L., Shang, Q.H., Xu, G.H., Wang, Y.Y., and Yang, J.S., 2018, High-precision temporal calibration of Middle Triassic vertebrate biostratigraphy: U-Pb zircon constraints for the *Sinokannemeyeria* Fauna and *Yonghesuchus*: Vertebrata PalAsiatica, v. 56, p. 16–24.

Liu, Y.Q., Kuang, H.W., Peng, N., Xu, H., Zhang, P., Wang, N.S., and An, W., 2015, Mesozoic basins and associated palaeogeographic evolution in North China: Journal of Palaeogeography, v. 4, p. 189–202, https://doi.org/10.3724/SP.J.1261.2015.00073.

Looy, C.V., Brugman, W.A., Dilcher, D.L., and Visscher, H., 1999, The delayed resurgence of equatorial forests after the Permian–Triassic ecologic crisis: Proceedings of the National Academy of Sciences of the United States of America, v. 96, p. 13,857–13,862, https://doi.org/10.1073/pnas.96.24.13857.

Looy, C.V., Twitchett, R.J., Dilcher, D.L., Van Konijnenburg-Van Cittert, J.H.A., and Visscher, H., 2001, Life in the end-Permian dead zone: Proceedings of the National Academy of Sciences of the United States of America, v. 98, p. 7879–7883, https://doi.org/10.1073/pnas.131218098.

Lu, J., Zhang, P.X., Yang, M.F., Shao, Y.L., and Hilton, J., 2020, Continental records of organic carbon isotopic composition ($\delta^{13}C_{org}$), weathering, paleoclimate and wildfire linked to the end-Permian mass extinction: Chemical Geology, v. 558, https://doi.org/10.1016/j.chemgeo.2020.119764.

Downloaded from http://pubs.geoscienceworld.org/gsa/gsabulletin/article-pdf/doi/10.1130/B36316.1/5749686/b36316.pdf
by University of Bristol user

Mays, C., Vajda, V., Frank, T., Fielding, C., Nicoll, R.S., Tevyaw, A., and McLoughlin, S., 2020, Refined Permian-Triassic floristic timeline reveals early collapse and delayed recovery of south polar terrestrial ecosystems: Geological Society of America Bulletin, v. 132, p. 1489–1513, https://doi.org/10.1130/B35355.1.

Mays, C., McLoughlin, S., Frank, T.D., Fielding, C.R., Slater, S.M., and Vajda, V., 2021a, Lethal microbial blooms delayed freshwater ecosystem recovery following the end-Permian extinction: Nature Communications, v. 12, p. 1–11, https://doi.org/10.1038/s41467-021-25711-3.

Mays, C., Vajda, V., and McLoughlin, S., 2021b, Permian–Triassic non-marine algae of Gondwana: Distributions, natural affinities and ecological implications: Earth-Science Reviews, v. 212, https://doi.org/10.1016/j.earscirev.2020.103382.

McLoughlin, S., 2001, The breakup history of Gondwana and its impact on pre-Cenozoic floristic provincialism: Australian Journal of Botany, v. 49, p. 271–300, https://doi.org/10.1071/BT00023.

McLoughlin, S., 2011, *Glossopteris*: Insights into the architecture and relationships of an iconic Permian Gondwanan plant: Journal of the Botanical Society of Bengal, v. 65, p. 1–14.

McLoughlin, S., Nicoll, R.S., Crowley, J.L., Vajda, V., Mays, C., Fielding, C.R., Frank, T.D., Wheeler, A., and Bocking, M., 2021, Age and paleoenvironmental significance of the Frazer Beach Member: A new lithostratigraphic unit overlying the end-Permian extinction horizon in the Sydney Basin, Australia: Frontiers of Earth Science, v. 8, https://doi.org/10.3389/feart.2020.600976.

Nesbitt, S.J., Liu, J., and Li, C., 2011, A sail-backed suchian from the Heshanggou Formation (Early Triassic: Olenekian) of China: Earth and Environmental Science Transactions of the Royal Society of Edinburgh, v. 101, p. 271–284, https://doi.org/10.1017/S1755691011020044.

Niklas, K.J., Tiffney, B.H., and Knoll, A.H., 1983, Patterns in vascular land plant diversification: Nature, v. 303, p. 614–616, https://doi.org/10.1038/303614a0.

Nowak, H., Schneebeli-Hermann, E., and Kustatscher, E., 2019, No mass extinction for land plants at the Permian–Triassic transition: Nature Communications, v. 10, no. 384, https://doi.org/10.1038/s41467-018-07945-w.

Ouyang, S., and Norris, G., 1988, Spores and pollen from the Lower Triassic Heshanggou Formation, Shaanxi Province, North China: Review of Palaeobotany and Palynology, v. 54, p. 187–231, https://doi.org/10.1016/0034-6667(88)90015-2.

Ouyang, S., and Wang, R.N., 1985, Age assignment of the Pingdingshan Member in Henan and Anhui provinces: Shiyou Shiyan Dizhi, v. 7, p. 141–147.

Ouyang, S., and Zhang, Z.L., 1982, Early Triassic palynological assemblage in Dengfeng, northwestern Henan: Acta Palaeontologica Sinica, v. 21, p. 685–696.

Pang, Q.Q., 1989, The Early–Middle Triassic stratigraphy and Ostracoda from the Yima area in Henan province: Journal of Hebei College of Geology, v. 12, p. 325–345.

Qu, L.F., 1980, Triassic spore and pollen fossils, *in* Institute of Geology and Chinese Academy of Geological Sciences, Mesozoic Stratigraphy and Paleontology of the Shaanxi-Gansu-Ningxia Basin: Beijing, China, Publishing House of Geology, v. 1, p. 115–143.

Qu, L.F., 1982, The palynological assemblage from the Liujiagou Formation of Jiaocheng, Shanxi. Bulletin of Geological Institute: Chinese Academy of Geological Society, v. 4, p. 83–93.

Qu, L.F., Yang, J.D., Bai, Y.H., and Zhang, Z.L., 1983, A preliminary discussion on the characteristics and stratigraphic divisions of Triassic spores and pollen in China: Bulletin Chinese Academy of Geological Sciences, v. 5, p. 81–94.

Rees, P.M., 2002, Land-plant diversity and the end-Permian mass extinction: Geology, v. 30, p. 827–830, https://doi.org/10.1130/0091-7613(2002)030<0827:LPDATE>2.0.CO;2.

Retallack, G.J., Veevers, J.J., and Morante, R., 1996, Global coal gap between Permian-Triassic extinction and Middle Triassic recovery of peat-forming plants: Geological Society of America Bulletin, v. 108, p. 195–207, https://doi.org/10.1130/0016-7606(1996)108<0195:GCGBPT>2.3.CO;2.

Schneebeli-Hermann, Hochuli, P.A., and Bucher, H., 2017, Palynofloral associations before and after the Permian–Triassic mass extinction, Kap Stosch, East Greenland: Global and Planetary Change, v. 155, p. 178–195.

Scotese, C.R., 2021, An Atlas of Phanerozoic Paleogeographic Maps: The seas come in and the seas go out: Annual Review of Earth and Planetary Sciences, v. 49, p. 679–728, https://doi.org/10.1146/annurev-earth-081320-064052.

Sephton, M.A., Jiao, D., Engel, M.H., Looy, C.V., and Visscher, H., 2015, Terrestrial acidification during the end-Permian biosphere crisis?: Geology, v. 43, p. 159–162, https://doi.org/10.1130/G36227.1.

Shen, W.J., Sun, Y.G., Lin, Y.T., Liu, D.H., and Chai, P.X., 2011, Evidence for wildfire in the Meishan section and implications for Permian–Triassic events: Geochimica et Cosmochimica Acta, v. 75, p. 1992–2006, https://doi.org/10.1016/j.gca.2011.01.027.

Shu, W.C., Tong, J.N., Tian, L., Benton, M.J., Chu, D.L., Yu, J.X., and Guo, W.W., 2018, Limuloid trackways from Permian-Triassic continental successions of North China: Palaeogeography, Palaeoclimatology, Palaeoecology, v. 508, p. 71–90, https://doi.org/10.1016/j.palaeo.2018.07.022.

Song, H.J., Wignall, P.B., Tong, J.N., Song, H.Y., Chen, J., Chu, D.L., Tian, L., Luo, M., Zong, K.Q., Chen, Y.L., Lai, X.L., Zhang, K.X., and Wang, H.M., 2015, Integrated Sr isotope variations and global environmental changes through the Late Permian to early Late Triassic: Earth and Planetary Science Letters, v. 424, p. 140–147, https://doi.org/10.1016/j.epsl.2015.05.035.

Stanley, S.M., 2016, Estimates of the magnitudes of major marine mass extinctions in earth history: Proceedings of the National Academy of Sciences of the United States of America, v. 113, p. E6325–E6334, https://doi.org/10.1073/pnas.1613094113.

Stevens, L.G., Hilton, J., Bond, D.P.G., Glasspool, I.J., and Jardine, P.E., 2011, Radiation and extinction patterns in Permian floras from North China as indicators for environmental and climate change: Journal of the Geological Society, v. 168, p. 607–619, https://doi.org/10.1144/0016-76492010-042.

Sun, Y.D., Joachimski, M.M., Wignall, P.B., Yan, C.B., Chen, Y.L., Jiang, H.S., Wang, L.N., and Lai, X.L., 2012, Lethally hot temperatures during the Early Triassic Greenhouse: Science, v. 338, p. 366–370, https://doi.org/10.1126/science.1224126.

Tong, J.N., Chu, D.L., Liang, L., Shu, W.C., Song, H.J., Song, T., Song, H.Y., and Wu, Y.Y., 2019, Triassic integrative stratigraphy and timescale of China: Science China. Earth Sciences, v. 62, p. 189–222, https://doi.org/10.1007/s11430-018-9278-0.

Tu, C.Y., Chen, Z.Q., Retallack, G.J., Huang, Y.G., and Fang, Y.H., 2016, Proliferation of MISS-related microbial mats following the end-Permian mass extinction in terrestrial ecosystems: Evidence from the Lower Triassic of the Yiyang area, Henan Province, North China: Sedimentary Geology, v. 333, p. 50–69, https://doi.org/10.1016/j.sedgeo.2015.12.006.

Vajda, V., McLoughlin, S., Mays, C., Frank, T.D., Fielding, C.R., Tevyaw, A., Lehsten, V., Bocking, M., and Nicoll, R.S., 2020, End-Permian (252 Mya) deforestation, wildfires and flooding: An ancient biotic crisis with lessons for the present: Earth and Planetary Science Letters, v. 529, https://doi.org/10.1016/j.epsl.2019.115875.

Visscher, H., Looy, C.V., Collinson, M.E., Brinkhuis, H., van Konijnenburg-van Cittert, J.H.A., Kürschner, W.M., and Sephton, M.A., 2004, Environmental mutagenesis during the end-Permian ecological crisis: Proceedings of the National Academy of Sciences of the United States of America, v. 101, p. 12,952–12,956, https://doi.org/10.1073/pnas.0404472101.

Wang, J., 2010, Late Paleozoic macrofloral assemblages from Weibei Coalfield, with reference to vegetational change through the Late Paleozoic Ice-age in the North China Block: International Journal of Coal Geology, v. 83, p. 292–317, https://doi.org/10.1016/j.coal.2009.10.007.

Wang, J., Liu, H.Q., Shen, G.L., and Zhang, H., 1998, Notes on the island distribution pattern of the Permian Cathaysian flora in China: An example of the application of the equilibrium theory of island biogeography in palaeobiogeography: Palaeogeography, Palaeoclimatology, Palaeoecology, v. 142, p. 23–31, https://doi.org/10.1016/S0031-0182(97)00147-8.

Wang, J.Y., Yi, J., and Liu, J., 2019, The first complete pareiasaur skull from China: Acta Palaeontologica Sinica, v. 58, p. 216–221.

Wang, L.X., 1983, Triassic of Shanxi: Shanxi Provincial Geological Prospecting Bureau, 198 pp.

Wang, L.X., Xie, Z.M., and Wang, Z.Q., 1978, On the occurrence of *Pleuromeia* from the Qinshui basin in Shanxi province: Acta Palaeontologica Sinica, v. 17, p. 195–211.

Wang, R.N., 1981, The "Shichienfeng Formation" of Yongcheng, Henan province and other adjacent area: Journal of Stratigraphy, v. 5, p. 180–189.

Wang, Z.Q., 1993, Evolutionary ecosystem of Permian–Triassic redbeds in North China: A historical record of global desertification: New Mexico Museum of Natural History and Science Bulletin, v. 3, p. 471–476.

Wang, Z.Q., 1996, Recovery of vegetation from the terminal Permian mass extinction in North China: Review of Palaeobotany and Palynology, v. 91, p. 121–142, https://doi.org/10.1016/0034-6667(95)00069-0.

Wang, Z.Q., and Wang, L.X., 1982, A new species of the lycopsid *Pleuromeia* from the early Triassic of Shanxi, China and its ecology: Palaeontology, v. 25, p. 215–225.

Wang, Z.Q., and Wang, L.X., 1986, Late Permian fossil plants from the lower part of the Shiqianfeng (Shihchienfeng) group in North China: Bulletin Tianjin Institute of Geology and Mineral Resources, v. 15, p. 1–120.

Wignall, P.B., 2015, The Worst of Times: How Life on Earth Survived Eighty Million Years of Extinctions: Princeton, New Jersey, USA, Princeton University Press, 224 p.

Wu, Q., Ramezani, J., Zhang, H., Wang, J., Zeng, F.G., Zhang, Y.C., Liu, F., Chen, J., Cai, Y.F., Hou, Z.S., Liu, C., Yang, W., Henderson, C.M., and Shen, S.Z., 2021, High-precision U-Pb age constraints on the Permian floral turnovers, paleoclimate change, and tectonics of the North China block: Geology, v. 49, p. 677–681, https://doi.org/10.1130/G48051.1.

Wu, Y.Y., Tong, J.N., Algeo, T.J., Chu, D.L., Cui, Y., Song, H.Y., Shu, W.C., and Du, Y., 2020, Organic carbon isotopes in terrestrial Permian-Triassic boundary sections of North China: Implications for global carbon cycle perturbations: Geological Society of America Bulletin, v. 132, p. 1106–1118, https://doi.org/10.1130/B35228.1.

Xiong, C.H., and Wang, Q., 2011, Permian–Triassic land-plant diversity in South China: Was there a mass extinction at the Permian/Triassic boundary?: Paleobiology, v. 37, p. 157–167, https://doi.org/10.1666/09029.1.

Xu, L., Li, X.W., Jia, S.H., and Liu, J., 2015, The Jiyuan tetrapod Fauna of the Upper Permian of China: New pareiasaur material and the reestablishment of *Honania complicidentata*: Acta Palaeontologica Polonica, v. 60, p. 689–700.

Xu, Z., Hilton, J., Yu, J.X., Wignall, P.B., Yin, H.F., Xue, Q., Ran, W.J., Hui, L., Shen, J., and Meng, F.S., 2022, Mid-Permian to Late Triassic plant species richness and abundance patterns in South China: Co-evolution of plants and the environment through the Permian-Triassic transition: Earth-Science Reviews, https://doi.org/10.1016/j.earscirev.2022.104136.

Yang, G.X., and Wang, H.S., 2012, Yuzhou Flora: A hidden gem of the Middle and Late Cathaysian Flora: Science China. Earth Sciences, v. 55, p. 1601–1619, https://doi.org/10.1007/s11430-012-4476-2.

Yin, H.F., and Lin, H.M., 1979, Marine Triassic faunas and the geologic time from Shihchienfeng Group in the northern Weihe River Basin, Shaanxi Province [in Chinese]: Acta Stratigraphica Sinica, v. 3, p. 233–241.

Yu, J.X., Broutin, J., Chen, Z.Q., Shi, X., Li, H., Chu, D.L., and Huang, Q.S., 2015, Vegetation changeover across the Permian–Triassic Boundary in Southwest China: Extinction, survival, recovery and palaeoclimate: A critical review: Earth-Science Reviews, v. 149, p. 203–224, https://doi.org/10.1016/j.earscirev.2015.04.005.

Yu, Y.Y., Tian, L., Chu, D.L., Song, H.Y., Guo, W.W., and Tong, J.N., 2022, Latest Permian–Early Triassic paleoclimatic reconstruction by sedimentary and isotopic analyses of paleosols from the Shichuanhe section in

Downloaded from http://pubs.geoscienceworld.org/gsa/gsabulletin/article-pdf/doi/10.1130/B36316.1/5749686/b36316.pdf
by University of Bristol user

central North China Basin: Palaeogeography, Palaeoclimatology, Palaeoecology, v. 585, https://doi.org/10.1016/j.palaeo.2021.110726.

Zheng, D., Chang, S.C., Wang, H., Fang, Y., Wang, J., Feng, C., Xie, G., Jarzembowski, E.A., Zhang, H., and Wang, B., 2018, Middle-Late Triassic insect radiation revealed by diverse fossils and isotopic ages from China: Science Advances, v. 4, https://doi.org/10.1126/sciadv.aat1380.

Zhu, R.K., Xu, H.X., Deng, S.H., and Guo, H.L., 2007, Lithofacies palaeogeography of the Permian in northern China: Journal of Palaeogeography, v. 9, p. 133–142.

Zhu, Z.C., Liu, Y.Q., Kuang, H., Benton, M.J., Newell, A.J., Xu, H., An, W., Ji, S.A., Xu, S.C., Peng, N., and Zhai, Q.G., 2019, Altered fluvial patterns in North China indicate rapid climate change linked to the Permian-Triassic mass extinction: Scientific Report, v. 9, https://doi.org/10.1038/s41598-019-53321-z.

Zhu, Z.C., Kuang, H., Liu, Y.Q., Benton, M.J., Newell, A.J., Xu, H., An, W., Ji, S.A., Xu, S.C., Peng, N., and Zhai, Q.G., 2020, Intensifying aeolian activity following the end-Permian mass extinction: Evidence from the Late Permian–Early Triassic terrestrial sedimentary record of the Ordos Basin, North China: Sedimentology, v. 67, p. 2691–2720, https://doi.org/10.1111/sed.12716.

Science Editor: Wenjiao Xiao
Associate Editor: Ganqing Jiang

Manuscript Received 1 September 2021
Revised Manuscript Received 26 July 2022
Manuscript Accepted 11 September 2022

Printed in the USA

Downloaded from http://pubs.geoscienceworld.org/gsa/gsabulletin/article-pdf/doi/10.1130/B36316.1/5749686/b36316.pdf
by University of Bristol user